Published in final edited form as:
J Comp Neurol. 2010 March 1; 518(5): 647–667. doi:10.1002/cne.22235.

Initial Loss but Later Excess of GABAergic Synapses with Dentate Granule Cells in a Rat Model of Temporal Lobe Epilepsy

Khushdev K. Thind[1], **Ruth Yamawaki**[1], **Ibanri Phanwar**[1], **Guofeng Zhang**[1], **Xiling Wen**[1], and **Paul S. Buckmaster**[1,2,*]

[1]Department of Comparative Medicine, Stanford University, Stanford, California 94305

[2]Department of Neurology & Neurological Sciences, Stanford University, Stanford, California 94305

Abstract

Many patients with temporal lobe epilepsy display neuron loss in the dentate gyrus. One potential epileptogenic mechanism is loss of GABAergic interneurons and inhibitory synapses with granule cells. Stereological techniques were used to estimate numbers of gephyrin-positive punctae in the dentate gyrus, which were reduced short-term (5 days after pilocarpine-induced status epilepticus) but later rebounded beyond controls in epileptic rats. Stereological techniques were used to estimate numbers of synapses in electron micrographs of serial sections processed for postembedding GABA-immunoreactivity. Adjacent sections were used to estimate numbers of granule cells and glutamic acid decarboxylase-positive neurons per dentate gyrus. GABAergic neurons were reduced to 70% of control levels short-term, where they remained in epileptic rats. Integrating synapse and cell counts yielded average numbers of GABAergic synapses per granule cell, which decreased short-term and rebounded in epileptic animals beyond control levels. Axo-shaft and axo-spinous GABAergic synapse numbers in the outer molecular layer changed most. These findings suggest interneuron loss initially reduces numbers of GABAergic synapses with granule cells, but later, synaptogenesis by surviving interneurons over-shoots control levels. In contrast, the average number of excitatory synapses per granule cell decreased short-term but recovered only toward control levels, although in epileptic rats excitatory synapses in the inner molecular layer were larger than in controls. These findings reveal a relative excess of GABAergic synapses and suggest that reports of reduced functional inhibitory synaptic input to granule cells in epilepsy might be attributable not to fewer but instead to abundant but dysfunctional GABAergic synapses.

Keywords

electron microscopy; gephyrin; stereology; interneuron; hippocampus; synaptogenesis

Temporal lobe epilepsy is common, can be difficult to treat, and is of unclear etiology (Engel et al., 1997). Patients display variable patterns and extents of neuron loss, but the hilus of dentate gyrus is particularly susceptible (Margerison and Corsellis, 1966). Many hilar neurons are GABAergic, and numbers of GABAergic interneurons are reduced in the dentate gyrus of patients with temporal lobe epilepsy (Sloviter et al., 1991; Mathern et al., 1995; Zhu et al., 1997; Maglóczky et al., 2000; Andrioli et al., 2007) and rodent models

*CORRESPONDENCE TO: Paul Buckmaster, Department of Comparative Medicine, 300 Pasteur Dr., R321 Edwards Building, Stanford University, Stanford, CA 94305. psb@stanford.edu.

The first two authors contributed equally.

(Obenaus et al., 1993; Buckmaster and Dudek, 1997; Buckmaster and Jongen-Rêlo, 1999; André et al., 2001; Gorter et al., 2001; Sayin et al., 2003; Boulland et al., 2007). One possible epileptogenic mechanism is the loss of GABAergic interneurons, which could reduce inhibition of dentate granule cells, thereby lowering seizure threshold. Consistent with this hypothesis, frequencies of miniature inhibitory postsynaptic currents (mIPSCs) in granule cells are reduced shortly after epileptogenic injuries and remain low in epileptic rats (Kobayashi and Buckmaster, 2003; Shao and Dudek, 2005; Sun et al., 2007; but see Leroy et al., 2004). These findings suggest that loss of inhibitory interneurons permanently reduces numbers of GABAergic synapses with granule cells, which reduces mIPSC frequency.

However, despite interneuron loss and reduced mIPSC frequency, it remains unclear whether numbers of GABAergic synapses with granule cells are reduced in temporal lobe epilepsy. Some measures of granule cell inhibition in epileptic dentate gyrus appear normal or enhanced (Haas et al., 1996; Isokawa, 1996; Bausch and Chavkin, 1997; Buckmaster and Dudek, 1999; Okazaki et al., 1999). Surviving interneurons might sprout axon collaterals and develop new GABAergic synapses with granule cells. There is evidence of interneuron axon sprouting; however, most is based on increased immunoreactivity of axons in tissue from patients (Babb et al., 1989; Mathern et al., 1995, 1999; Patrylo et al., 1999; Arellano et al., 2004) and rodent models (Davenport et al., 1990; Schwarzer et al., 1995; Houser and Esclapez, 1996; Bausch and Chavkin, 1997; Mathern et al., 1997; Esclapez and Houser, 1999; André et al., 2001; Boulland et al., 2007). Preexisting axons may become more visible in epileptic tissue because antigen expression is upregulated. Even if there were axon sprouting, synaptogenesis does not necessarily follow. Limited but more direct electron microscopic evidence is consistent with GABAergic synaptogenesis (Wittner et al., 2001).

Thus, whether dentate granule cells receive fewer GABAergic synapses shortly after epileptogenic injuries and later in epileptic tissue remains unresolved. Reduced frequency of mIPSCs in granule cells of epileptic animals might be attributable to fewer GABAergic synapses, reduced release probability, or both. It is important to distinguish between these alternatives, because each requires different treatments. To determine whether inhibitory synapses decrease after an epileptogenic treatment and recover later in epileptic animals, we used stereological techniques to estimate numbers of GABAergic synapses per granule cell in a rat model of temporal lobe epilepsy. Excitatory synapses also were evaluated.

MATERIALS AND METHODS

Animals

All experiments were performed in accordance with the National Institutes of Health *Guide for the Care and Use of Laboratory Animals* and approved by the Stanford University Institutional Animal Care and Use Committee. Male 35 ± 2-day-old Sprague–Dawley rats (Harlan, Indianapolis, IN) were treated with pilocarpine as described previously (Buckmaster, 2004). Briefly, pilocarpine (380 mg/kg, i.p.) was administered 20 minutes after atropine methyl bromide (5 mg/kg, i.p.). Diazepam (Hospira, Lake Forest, IL) was administered (10 mg/kg, i.p.) 2 hours after the onset of Stage 3 or greater seizures (Racine, 1972) and repeated as necessary to suppress convulsions. Control rats included age-matched naïve rats and animals that were treated with pilocarpine but did not develop status epilepticus and epilepsy. There were no significant differences between control groups, so the results were combined (see Results). Video monitoring, which began at least 10 days after pilocarpine treatment, verified spontaneous motor convulsions in all epileptic rats. No controls were observed to have spontaneous seizures.

Tissue processing

Gephyrin immunoreactivity was evaluated in three groups: pilocarpine-treated controls (n = 6), rats 5 days after status epilepticus (n = 6), and epileptic rats (n = 6) 83 ± 3 days after status epilepticus (108 ± 4 days old at perfusion). Animals were evaluated 5 days after status epilepticus to allow time for synapses to degenerate after status epilepticus-induced neuron loss but to precede the onset of extensive, reactive synaptogenesis. Rats were killed with urethane (2 g/kg i.p.) and lightly fixed by perfusion through the ascending aorta at 30 mL/min for 2 minutes with 0.9% sodium chloride and for 10 minutes with 4% paraformaldehyde in 0.1 M phosphate buffer (PB, pH 7.4) at 4°C. Brains were postfixed for 1 hour at 4°C, then equilibrated in 30% sucrose in PB at 4°C. Right hippocampi were isolated and stored at −80°C. Hippocampi were thawed in 30% sucrose in PB, gently straightened, frozen, and sectioned perpendicular to septotemporal axis with a sliding microtome set at 40 μm. Sections were stored at −20°C in 30% ethylene glycol and 25% glycerol in 50 mM PB. Beginning at a random starting point near the septal pole and extending through the entire septotemporal length, a 1-in-24 series of sections was rinsed in PB and mounted on gelatin-coated microscope slides. Tissue was processed in batches that included balanced numbers of animals from each experimental group. Sections were rinsed in 0.1 M Tris-buffered saline (TBS, pH 7.4) and placed for 2 hours in blocking solution consisting of 3% goat serum, 2% bovine serum albumin (BSA), and 0.3% Triton X-100 in 0.05 M TBS. After rinsing in TBS, sections incubated overnight at 4°C in 1% goat serum, 0.2% BSA, 0.3% Triton X-100, 0.05 M TBS, and gephyrin antiserum (Table 1). Sections were rinsed in TBS and incubated for 3 hours in 2% BSA, 0.3% Triton X-100, 0.05 M TBS, and 10 μg/mL Alexa Fluor 488 goat antimouse serum (Invitrogen, Carlsbad, CA). Sections were rinsed in TBS and coverslipped with Vectashield (Vector Laboratories, Burlingame, CA).

Electron microscopy, Nissl staining, and in situ hybridization were evaluated in another set of rats consisting of three groups: controls (n = 6), rats 5 days after status epilepticus (n = 3), and epileptic rats (n = 5) 101 ± 60 days after status epilepticus (172 ± 31 days old at perfusion). Rats were killed with urethane (2 g/kg i.p.) and perfused through ascending aorta at 30 mL/min for 1 minute with 0.9% sodium chloride and 30 minutes with 2.5% paraformaldehyde and 1% glutaraldehyde in 0.1 M PB (pH 7.4) at 4°C. Brains were postfixed overnight at 4°C. Left hippocampi were isolated, equilibrated in 30% sucrose in PB at 4°C, gently straightened, frozen, and sectioned perpendicular to septotemporal axis with a sliding microtome set at 40 μm. Beginning at random starting points near the septal pole and extending through the entire septotemporal length, 1-in-12 series of sections were Nissl-stained with 0.25% thionin. Other 1-in-12 series of sections were stored at −20°C in 30% ethylene glycol and 25% glycerol in 50 mM PB and later processed for in situ hybridization for glutamic acid decarboxylase-65 (GAD). GAD65-cDNA (kindly provided by Drs. A. Tobin and N. Tillakaratne, University of California at Los Angeles) was ≈2.3 kb, isolated from a λ ZapII library from adult rat hippocampus (Erlander et al., 1991), and included the entire coding region (≈1,755 bp), ≈74 bp of the 5′ untranslated region, and ≈467 bp of the 3′ untranslated region (Dr. N. Tillakaratne, University of California at Los Angeles, pers. commun.). RNA probes were produced by transcription of GAD65-cDNA using a nonradioactive RNA labeling kit (Roche, Indianapolis, IN). Sections were washed in 10 mM phosphate-buffered saline (PBS) and incubated sequentially in 0.02 N HCl, 0.01% Triton X-100 in PBS, 0.2 μg/mL proteinase K (Roche) in 50 mM Tris (pH 7.4), 5 mM EDTA, and 2 mg/mL glycine (Roche) in PBS. Sections were prehybridized for 1 hour in a solution containing 50% formamide, 750 mM NaCl, 25 mM EDTA, 25 mM piperazine-*N*,*N*'-bis 2-ethanesulfonic acid (Roche), 0.2% sodium do-decyl sulfate, 250 μg/mL poly A (Roche), and 250 μg/mL salmon sperm DNA (Roche). Sections were hybridized for 2 days in a humid chamber at 50°C in a solution consisting of the prehybridization solution with digoxygenin-labeled RNA probe at a concentration of 2–4 μL/mL, 100 mM dithiothreitol,

4% dextran sulfate, and 250 μg/mL tRNA (Roche). After hybridization, sections were subjected to RNase treatment and stringency washes. Sections were processed for immunodetection of digoxygenin label with reagents of a nonradioactive nucleic acid detection kit (Roche), mounted on gelatin-coated slides, and cover-slipped with Crystalmount (Biomedia, Foster City, CA) and Permount.

Other 1-in-12 series of sections from the same hippocampi from which sections were obtained for Nisslstaining and GAD in situ hybridization were prepared for electron microscopy. Sections were postfixed with 1% OsO_4 in sodium cacodylate buffer (pH 7.2) for 1 hour, dehydrated in a series of ethanols, placed in propylene oxide, gradually transferred to pure Araldite/Eponate-12 (Ted Pella, Redding, CA), and flat-embedded between sheets of ACLAR at 60°C for 24 hours. Sample areas on flatembedded tissue sections were isolated and mounted on blank epoxyresin capsules. Block faces were trimmed and ultrathin sections of silver interference color were cut from reembedded blocks with an ultramicrotome (Reichert Ul-tracut S, Leica, Vienna, Austria). Serial sections were collected on coated, nickel single-slot grids. Postembedding GABA-immunocytochemistry was performed on ultrathin sections by blocking nonspecific labeling with 0.8% ovalbumin and 5% fetal calf serum in 0.05 M TBS (pH 7.6) for 1 hour followed by incubation overnight in GABA antiserum (Table 1) in blocking solution. Grids were gently rinsed and then incubated in antirabbit colloidal gold (10-nm-diameter, 1:80, Ted Pella) in 0.1% Triton X-100 and 0.05 M Tris buffer (pH 8.2) for 90 minutes. Sections were post-stained with 2% aqueous uranyl acetate for 6 minutes and Sato's lead stain for 4 minutes.

Antibody characterization

Please see Table 1 for a list of all antibodies used. The gephyrin antibody stains a major band of 93 kD molecular weight and a minor band of 48 kD on Western blot of purified gephyrin, but is not sensitive enough to pick up these proteins in Western blots of rat brain tissue (manufacturer's technical information). Electron microscopic analysis of rat dentate gyrus revealed that gephyrin antiserum was colocalized with symmetric postsynaptic densities. Specificity of the GABA antiserum was suggested by its pattern of labeling, for example, of axon terminals that formed symmetric synapses (Figs. 3A–K, 4A–C). Axon terminals that form symmetric synapses have been reported to be GABAergic structures in the dentate gyrus of rats (Kosaka et al., 1984; Halasy and Somogyi, 1993a). Electron microscopic analysis revealed that preadsorption with BSA did not block specificity of staining, suggesting the antiserum detected GABA, not BSA.

Analysis

Investigators were blind to experimental groups during analysis. The optical fractionator method (West et al., 1991) was used as described previously to estimate numbers of neurons (Buckmaster and Jongen-Rêlo, 1999) and immunoreactive punctae (Kumar and Buckmaster, 2006). Sampling parameters are listed in Table 2. To estimate total numbers of gephyrin-immunoreactive punctae in the granule cell layer plus molecular layer of the dentate gyrus, borders were outlined in sections and sample sites determined randomly and systematically with Stereo Investigator software (MBF Bioscience, Williston, VT). Sample site locations in the granule cell layer, inner third of the molecular layer, or outer two-thirds of the molecular layer were recorded on low-magnification images of sections. Landmarks in the tissue that were visible in low-magnification images were used to relocate sample sites and collect high-magnification images with a confocal laser-scanning microscope (LSM 5 Pascal, Zeiss, Oberkochen, Germany) equipped with a 100× objective and set at 10× zoom. An average of 3,230 ± 373 gephyrin-immunoreactive punctae were counted per rat. A total of 58,140 gephyrin-positive punctae were counted at 1,469 sample sites in 162 sections from 18 rats. To estimate punctae numbers per dentate gyrus, fractions of area sampled were calculated

by multiplying numbers of sample sites by counting frame area and dividing by total areas of analyzed regions per section. Gephyrin-positive punctae were counted within sample sites, which consisted of image stacks (6 × 0.4 μm separation). All gephyrin-positive punctae were counted unless they were visible in the most superficial section of a stack or touched left or bottom borders of counting frames. The superficial guard zone was the most superficial section of the stack. Beneath the analyzed stack, an additional optical section was included to provide a deep guard zone.

To estimate numbers of GAD-positive neurons per dentate gyrus, Nissl-stained granule cells, and Nissl-stained hilar neurons, sample sites were randomly and systematically determined by Stereo Investigator software (MBF Bioscience) within borders drawn around corresponding regions: entire dentate gyrus, granule cell layer, and hilus, respectively. The hilus was defined by its border with the granule cell layer and straight lines drawn from the ends of the granule cell layer to the proximal end of the CA3 pyramidal cell layer. The dentate gyrus was defined by the hilar border with CA3 and by the edge of the molecular layer, which was the edge of the tissue in the inferior blade and the hippocampal fissure in the superior blade. Total section thickness was used for dissector height, and only labeled somata or nuclei that were not cut at the upper surfaces of sections were counted. This modification of the optical fractionator method facilitates analysis of tissue sectioned thinly to enhance staining; however, it might increase the probability of underestimating cell numbers. There would be no effect on relative values of control versus other groups, because all were analyzed identically. GAD-positive somata and large Nissl-stained nuclei (neuronal, not glial) in the granule cell layer and hilus were counted using a 100× objective. A total of 3,135 granule cells were counted at 1,029 sample sites in 156 sections from 14 rats (224 ± 10 counted granule cells/rat). In the same sections, 7,104 Nissl-stained neurons were counted at 3,456 sample sites in the hilus (507 ± 41 counted hilar neurons/rat). A total of 3,475 GAD-positive neurons were counted at 10,605 sample sites in 156 sections in the entire dentate gyrus (248 ± 20 counted GAD-positive neurons/rat).

To estimate numbers of synapses in the dentate gyrus, we modified a stereological method developed originally to estimate total numbers of synapses in stratum radiatum of the CA1 field in hippocampus (Geinisman et al., 1996, 2000). Parameters of the stereological electron microscopic synapse counts are listed in Table 3. To measure areas of strata within the dentate gyrus, embedded sections were analyzed with Neurolucida (MBF Bioscience) and a microscope (Nikon, Melville, NY) equipped with a 10× objective, and Lucivid (MBF Bioscience). Contours were drawn around the granule cell layer, inner third of the molecular layer, and outer two-thirds of the molecular layer. Borders between the inner third and outer molecular layer were determined by measuring total height of the molecular layer and placing a series of points one-third of the way from the granule cell layer toward the outer border of molecular layer. As in previous studies (Geinisman et al., 1996, 2000), six sites per hippocampus were sampled for electron microscopy. To ensure that synapses in all parts of the dentate gyrus had equal probability of being sampled, sample sites were distributed systematically and randomly. For each animal, cumulative length of the granule cell layer was measured and divided into six uniform intervals. Placements of first sample sites were randomly located within first intervals, and subsequent samples were at equal intervals. For example, Figure 1 shows the 12 embedded sections of a control rat. For each section, granule cell layer length was measured beginning at the tip of the superior blade to the apex and then to the tip of the inferior blade. In this example the cumulative length of the granule cell layer was 73.7 arbitrary units, which was divided by 6, yielding 12.3. A random number between 0 and 12.3 was generated (2.8, in this case), and the first sample site was 2.8 units from the starting point, which was the tip of superior blade of the granule cell layer in the first section. The next sample point was 12.3 units farther along the granule cell layer, which extended through the rest of the granule cell layer in the first section and the granule cell

layer length of the second section and was located in the inferior blade of the granule cell layer in the third section. The next sample point was 12.3 units farther along the granule cell layer, and so on, until six sample sites were identified. At each sample site, tissue was trimmed to include the entire height of the molecular layer and granule cell layer. For each hippocampus, the fraction of area sampled was calculated by multiplying the number of sample sites per stratum (six) by counting frame area and dividing by area of that stratum.

At each sample site, counting frames were located in the granule cell layer, inner molecular layer, and outer molecular layer. Counting frames were randomly determined by locations of score marks made by small imperfections in the cutting edges of diamond knives used to make ultrathin sections. Low-magnification electron micrographs were used to verify score-mark locations. Counting frames were the area of electron micrographs (3.69 × 5.11 μm) photographed using a transmission electron microscope (JEOL 100CX; JEOL, Peabody, MA) at 25,000× magnification and printed at a final magnification of 48,400×. Counting frames were aligned across 100 consecutive ultrathin sections for the inner and outer molecular layer and 150 consecutive sections in the granule cell layer, where synapse density is lower. Counting frames were aligned at one axis by the edge of the tissue block and at the other axis by a score-mark. These fiduciary marks were determined without bias and were independent of tissue-based landmarks. Between fiduciary marks and photographed areas there were borders of constant dimensions, so tissue within photographed areas was not disrupted. Tissue samples were sectioned completely, and total numbers of ultrathin sections determined, so sampled fractions of tissue thickness could be calculated.

Collecting large series of consecutive ultrathin sections and processing them for postembedding immunocytochemistry is technically demanding. Occasional sections were damaged or lost. If five or more consecutive sections were unavailable for analysis in a series, an equal number was added to the end of the series to compensate. This occurred an average of 0.48 times per series, and there were no significant differences between experimental groups ($P = 1$, analysis of variance [ANOVA]). Gaps consisting of four or fewer consecutive sections also occurred: 78% one section, 14% two sections, 5% three sections, and 3% four sections. An average of eight sections per series was missing, and there were no significant differences between experimental groups ($P = 0.48$, ANOVA). These missing sections were not compensated, because gaps were small relative to synapse size, making it unlikely that synapses were missed.

Synapses were identified by parallel membranes, concentration of presynaptic vesicles, and postsynaptic densities (Gray, 1959). All synapses that appeared at least partially within fields of view in series of consecutive sections were counted, unless they were evident in the first section of a series or touched the upper or left-hand borders of prints. The superficial guard zone was the most superficial ultrathin section of the series. Beneath the analyzed series, additional ultrathin sections were included to provide a deep guard zone.

GABA-immunoreactive structures were identified by comparing densities of gold particles to background levels. Pilot tests verified the specificity of GABA labeling. The density of colloidal gold particles was measured over a series of representative sections containing putative GABA-negative and GABA-positive axon terminals and dendrites in the molecular layer. Putative GABA-positive axon terminals were identified by the presence of a symmetric synapse. Putative GABA-negative axon terminals were identified by the presence of an asymmetric synaptic contact with a dendritic spine. Putative GABA-positive dendrites were identified by a high density of asymmetric synaptic contacts with an aspiny dendritic shaft. Putative GABA-negative dendrites were identified by the presence of spines. Using a Neurolucida system (MBF Bioscience) equipped with a data tablet, areas of these structures

and the numbers of gold particles overlying them were measured. Gold particle density was highest in putative GABA-positive axon terminals and lowest in putative GABA-negative axon terminals. Relative gold particle densities were 1.0 in GABA-negative axon terminals, 1.4 in GABA-negative dendrites; 10.5 in GABA-positive dendrites, and 28.8 in GABA-positive axon terminals. Therefore, the postembedding GABA immunocytochemistry protocol labeled GABA-positive axons and dendrites with intensities over 10-fold higher than background levels. This level of labeling specificity obviated the need for measuring gold particle density in all of the electron micrographs.

Postsynaptic structures were identified by neurochemical (GABA-negative or GABA-positive) and ultrastructural characteristics. Ultrastructural characteristics included microtubules and mitochondria for dendritic shafts; a spine apparatus, and lack of other organelles for dendritic spines; a nucleus and organelles, including Golgi apparatus, for somata; and microtubule fascicles and membrane undercoating for axon initial segments (Peters et al., 1991).

Sizes of GABA-negative asymmetric synapses were measured for a randomly sampled subset of counted synapses whose postsynaptic densities were within or touchinga1 × 1 μm area centered in counting frames of entire series except the last 25 prints. Lengths of postsynaptic densities were measured in each section, summed, and multiplied by ultrathin section thickness to yield synapse area.

Totals of 16,335 GABA-positive and 43,023 GABA-negative synapses (1,167 ± 103 and 3,073 ± 184 per rat, respectively) were counted at 252 sample points consisting of over 29,000 electron micrographs from 14 rats. GABA-negative synapse size was measured at 3,157 synapses (226 ± 12 per rat).

Images were prepared using Adobe Photoshop (San Jose, CA). Only brightness and contrast were adjusted. All chemicals and drugs were obtained from Sigma (St. Louis, MO) unless specified otherwise. Results are reported as mean ± SEM. Statistics were performed using Sigma Stat (Systat, San Jose, CA) with $P < 0.05$ considered significant.

RESULTS

Initial loss and later rebound of gephyrin-immunoreactive punctae

Gephyrin-immunoreactive punctae are postsynaptic markers of GABAergic synapses (Craig et al., 1996). Randomly and systematically sampled hippocampal sections from controls, rats 5 days after status epilepticus, and epileptic rats (n = 6/group) were analyzed. Similar to previous studies (Simbürger et al., 2000), intensity of gephyrin staining was low in the granule cell layer and greatest in the outer molecular layer (Fig. 2A). Normally, rat granule cell somata are located almost exclusively in the granule cell layer, and their dendrites extend almost exclusively into the molecular layer. Therefore, to evaluate synapses with granule cells, the granule cell layer and molecular layer, but not the hilus, were analyzed. Stereological methods were used to estimate total numbers of gephyrin-positive punctae per dentate gyrus (not hilus) (Table 2). The average number of gephyrin-immunoreactive punctae per dentate gyrus in controls was 1.99 (± 0.13) × 10^9 (Fig. 2D). The average number of gephyrin-immunoreactive punctae per dentate gyrus was significantly reduced to 1.40 (± 0.16) × 10^9 (70% of control levels) in rats 5 days after status epilepticus and significantly increased to 2.50 (± 0.17) × 10^9 (126% of control levels) in epileptic rats ($P < 0.05$, ANOVA, Student–Newman–Keuls method).

The temporal end of the hippocampus is suspected to be particularly important in temporal lobe epilepsy, in part because it is the region that when surgically resected usually reduces

seizure frequency in patients (Engel et al., 1997). Numbers of gephyrin-positive punctae in the part of the temporal hippocampus sampled by the three most temporal sections of each hippocampus were calculated. The average number of gephyrin-positive punctae in the temporal dentate gyrus was 2.38 million in controls. It was reduced to 1.72 million in rats 5 days after status epilepticus (72% of controls) and was increased to 2.86 million in epileptic rats (120% of controls). Thus, proportional changes in the temporal dentate gyrus were similar to that of the entire dentate gyrus.

GABAergic synaptic input overlaps strata-specific areas of excitatory synaptic input to granule cells (Han et al., 1993). Layer II neurons in the lateral and medial entorhinal cortex target the outer and middle thirds of the molecular layer, respectively (Steward, 1976). Commissural/associational input from hilar mossy cells targets the inner molecular layer (Berger et al., 1980; Buckmaster et al., 1996), which also receives aberrant input from granule cells in epileptic tissue (Nadler et al., 1980a; Buckmaster et al., 2002b). Therefore, to more precisely determine where changes occurred, numbers of gephyrin-immunoreactive punctae were expressed by strata (Fig. 2E). In controls, the fewest gephyrin-immunoreactive punctae were in the granule cell layer ($0.26 (\pm 0.01) \times 10^9$, 13% of total), and most were in the outer molecular layer ($1.37 (\pm 0.01) \times 10^9$, 69% of total). Differences between strata were significant ($P < 0.001$, ANOVA). Although total numbers varied, distributions across strata were similar in all experimental groups. These findings suggest that across all strata but mostly in the outer molecular layer there may be loss of GABAergic synapses with granule cells by 5 days after status epilepticus, and synapses may be restored to excess later in epileptic animals.

Gephyrin clusters at a substantial fraction of GABAergic synapses, but some are devoid of immunoreactivity (Sassoe-Pagnetto et al., 2000; Simbürger et al., 2001). Therefore, gephyrin punctae counts underestimate GABAergic synapse numbers. In addition, gephyrin-immunoreactivity is sensitive to aldehyde fixation (Kirsch and Betz, 1993). However, precautions were taken to avoid that potentially confounding effect (see Materials and Methods). Furthermore, as with other immunocytochemical markers, gephyrin expression levels may be affected by seizure activity. Therefore, to more accurately estimate GABAergic synapse numbers and identify their postsynaptic targets, we used electron microscopy (EM) of serial sections.

GABAergic synapses per dentate gyrus

To evaluate GABAergic synapses and their targets more specifically, another set of controls (n = 6), rats 5 days after status epilepticus (n = 3), and epileptic animals (n = 5) was evaluated. In this set, synapses were identified by serial section EM (Fig. 3A–J). GABAergic synapses were identified by parallel membranes, postsynaptic densities, which usually were thin (symmetric), and GABA-immunoreactive presynaptic boutons containing concentrations of synaptic vesicles. In rare cases, thick, asymmetric densities were found at GABAergic synapses, similar to previous reports in control rats (Kosaka et al., 1984; Halasy and Somogyi, 1993a). Numbers of GABAergic synapses per dentate gyrus were estimated using stereological sampling parameters listed in Table 3. The average number of GABAergic synapses per dentate gyrus (not hilus) in controls was $3.30 (\pm 0.42) \times 10^9$ (Fig. 3L). Comparing EM and gephyrin results suggests 61% of EM-identified GABAergic synapses were gephyrin-positive in the dentate gyrus of control rats. The average number of GABAergic synapses per dentate gyrus was reduced to $1.89 (\pm 0.40) \times 10^9$ (57% of control levels) in rats 5 days after status epilepticus and significantly increased to $4.84 (\pm 0.92) \times 10^9$ (147% of control levels) in epileptic rats ($P < 0.05$, ANOVA, Student–Newman–Keuls method).

GABAergic synapses were distributed across strata of dentate gyrus similar to gephyrin-immunoreactive punctae (Fig. 3M). In controls, the fewest GABAergic synapses were in the granule cell layer (0.24 (± 0.01) × 10^9, 13% of total) and most were in the outer molecular layer (1.23 (± 0.23) × 10^9, 65% of total). Differences between strata were significant ($P < 0.001$, ANOVA). Although total numbers varied, generally similar distributions across strata were found in all experimental groups. The greatest proportional losses and rebounds of GABAergic synapses occurred in the outer molecular layer, and smallest changes occurred in the granule cell layer. Similar to gephyrin immunocytochemistry results, these findings suggest that by 5 days after status epilepticus granule cells might lose GABAergic synaptic input, which is later restored to excess in epileptic animals.

Granule cell numbers and loss of hilar neurons and GABAergic interneurons

To reveal GABAergic synapse numbers on a per-cell basis, sections adjacent to those processed for EM were used to estimate numbers of hilar neurons, granule cells, and GABAergic interneurons per dentate gyrus (Fig. 4A–F). For estimates of all cell types, mean coefficients of error (0.046 – 0.085) were much less than coefficients of variation (0.164 – 0.308) (Table 2), suggesting sufficient sampling within available material (West et al., 1991). Similar to previous studies (West et al., 1991), the average number of granule cells per dentate gyrus in controls was 1.10 ± 0.06 million (Fig. 4G). Although they are relatively resistant, status epilepticus kills some granule cells (Obenaus et al., 1993; Sloviter et al., 1996a). Thus, in rats 5 days after status epilepticus, granule cell numbers were reduced to 0.90 ± 0.02 million (80% of control levels), but the difference was not statistically significant ($P = 0.10$, ANOVA). Later, in epileptic rats, granule cell numbers had recovered to 1.14 ± 0.09 million (103% of control levels). These findings suggest status epilepticus might have killed some granule cells, which later might have been replaced by neurogenesis (Parent et al., 1997).

Similar to previous studies (West et al., 1991; Buckmaster and Jongen-Rêlo, 1999), the average number of Nissl-stained hilar neurons per dentate gyrus in controls was 47,300 ± 2,200 (Fig. 4H). In rats 5 days after status epilepticus, hilar neurons were reduced to 21,500 ± 2,600 (46% of control levels) ($P < 0.05$ ANOVA, Student–Newman–Keuls method) and many glia were evident in the hilus (Fig. 4C). Later, in epileptic rats, hilar neuron numbers had increased significantly to 36,800 ± 3,600 (78% of control levels) but still remained significantly less than controls ($P < 0.05$, ANOVA, Student–Newman–Keuls method). These findings suggest status epilepticus killed many hilar neurons by 5 days after status epilepticus, replicating a common pathological feature found in patients with temporal lobe epilepsy (Margerison and Corsellis, 1966). Partial rebound of hilar neuron numbers in epileptic rats might be attributable to status epilepticus-induced generation of displaced granule cells (McCloskey et al., 2006).

GABAergic interneurons were identified with in situ hybridization for GAD65, which is a sensitive detection method (Obenaus et al., 1993; Houser and Esclapez, 1996). Tissue had been fixed for EM, and consequently in situ hybridization produced various degrees of background staining. However, background staining was not consistently elevated in any single group. In all cases, GAD-positive neurons could be identified clearly, and labeling was visible throughout section thickness. Similar to previous studies (Buckmaster and Jongen-Rêlo, 1999), the average number of GAD-positive neurons per dentate gyrus was 34,000 ± 1,900 (Fig. 4I). In rats 5 days after status epilepticus, GAD-positive neuron numbers were reduced to 23,900 ± 1,800 (70% of control levels) and remained at 24,100 ± 1,100 (71% of control levels) in epileptic rats ($P < 0.05$, ANOVA, Student-Newman-Keuls method). These findings suggest that ≈30% of GABAergic interneurons were killed by status epilepticus without later recovery or further loss in epileptic rats.

GABAergic synapses per granule cell

As described above, numbers of gephyrin-immunoreactive punctae and GABAergic synapses per dentate gyrus suggest individual granule cells lose GABAergic synapses by 5 days after status epilepticus, which may be restored to excess later in epileptic animals. This hypothesis was tested more precisely by estimating numbers of GABAergic synapses per granule cell. The number of GABAergic synapses with GABA-negative targets per dentate gyrus was divided by the number of granule cells per dentate gyrus for each rat. The underlying assumption that all GABA-negative synaptic targets in the granule cell layer and molecular layer were granule cells is not strictly correct. Some glutamatergic mossy cells extend dendrites into the granule cell layer and molecular layer, but that is rare in rats (Buckmaster et al., 1992). The average number of GABAergic synapses per granule cell in controls was 2,980 ± 400 (Fig. 5D). Average numbers of GABAergic synapses per granule cell were not significantly different in naïve (2,320 ± 570, n = 2) and pilocarpine-treated controls (3,320 ± 480, n = 4, $P = 0.28$, *t*-test) and results were combined for comparison with other experimental groups. In rats 5 days after status epilepticus, numbers of GABAergic synapses per granule cell were reduced to 2,110 ± 210 (71% of control levels) ($P < 0.05$ ANOVA, Student–Newman–Keuls method). Later, in epileptic rats, GABAergic synapses per granule cell had increased to 4,150 ± 610 (139% of control levels).

To determine where changes occurred, numbers of GABAergic synapses per granule cell were evaluated by dentate gyrus strata (Fig. 5E). The average number of GABAergic synapses per granule cell in controls was 329 ± 43 in the granule cell layer, 516 ± 55 in the inner third molecular layer, and 2,138 ± 320 in the outer molecular layer. Although total numbers varied, distributions among strata were similar in all experimental groups, with fewest synapses in the granule cell layer and most in the outer molecular layer. The average number of synapses per granule cell in the outer molecular layer differed most among groups, with rats 5 days after status epilepticus having only 1,373 ± 119 (52% of control levels) and epileptic animals having 3,143 ± 502 (136% of controls) ($P < 0.05$, ANOVA, Student–Newman–Keuls methods). These findings suggest granule cells receive most GABAergic synapses in the outer molecular layer, where initial loss after status epilepticus is most profound and later proliferation is greatest.

GABAergic synapses target different subcellular regions of granule cells (Halasy and Somogyi, 1993b), which is likely to have different functional effects (Miles et al., 1996). Granule cells receive GABAergic synapses on their axon initial segment and cell body (Kosaka et al., 1984), inner molecular layer dendrites (Han et al., 1993), and outer molecular layer dendrites. Many GABAergic synapses in the outer molecular layer are with spines that also receive a glutamatergic synapse (Fifkova et al., 1992). To more precisely determine where changes occurred, numbers of GABAergic synapses were evaluated by subcellular target (Fig. 5A–C). On average, control granule cells received 12 ± 3 axo-axonic, 190 ± 18 axo-somatic, 1490 ± 200 axo-shaft, and 1,290 ± 200 axo-spinous GABAergic synapses (Fig. 5F). Numbers of axo-axonic synapses may have been underestimated in the present study, because granule cell axons extend into hilus, which was not analyzed. Although total numbers varied, distributions among subcellular targets were similar in all experimental groups. The average number of axo-axonic synapses per granule cell increased to 20 ± 6 in epileptic rats, but the difference was not statistically significant. The average number of axo-shaft synapses increased significantly in epileptic animals to 2,290 ± 250 (154% of control levels) ($P < 0.05$, ANOVA, Student–Newman–Keuls methods). Axo-spinous synapses at 5 days after status epilepticus were only 649 ± 83 (50% of control levels) ($P < 0.05$, ANOVA, Student–Newman–Keuls methods) and increased to 1,700 ± 360 (131% of control levels) in epileptic rats. These findings suggest GABAergic synapse loss 5 days after status epilepticus is attributable mostly to loss of axo-spinous synapses, whereas axo-spinous and axo-shaft synapses proliferated most in epileptic rats.

Excitatory synapses per granule cell

To test whether GABA-negative, presumably glutamatergic, synapse numbers per granule cell changed, the same material and a similar stereological approach was used. However, only the inner and outer molecular layer were analyzed, because in control rats glutamatergic synapses in granule cell layer account for <0.5% of GABA-negative synapses in dentate gyrus (Halasy and Somogyi, 1993a). Putative glutamatergic synapses were identified by parallel membranes, thick (asymmetric) postsynaptic densities, and GABA-negative presynaptic boutons containing concentrations of synaptic vesicles (Fig. 6A–C). Some afferents from subcortical regions form GABA-negative asymmetric synapses with granule cells, and it is unclear whether they are glutamatergic (Maglóczky et al., 1994). Nevertheless, it is likely that the vast majority of GABA-negative synapses with granule cells are glutamatergic. The average number of GABA-negative synapses per granule cell in controls was 10,800 ± 1,000 (Fig. 6D). Average numbers of GABA-negative synapses per granule cell were similar in naïve (10,300 ± 400, n = 2) and pilocarpine-treated controls (11,000 ± 1,600, n = 4, $P = 0.77$, *t*-test), and results were combined for comparison with other experimental groups. In rats 5 days after status epilepticus, the average number of GABA-negative synapses per granule cell was reduced to 6,600 ± 100 (61% of control levels) ($P < 0.05$ ANOVA, Student–Newman–Keuls method). Later, in epileptic rats, GABA-negative synapses per granule cell had recovered to 10,400 ± 800 (97% of control levels). These findings suggest granule cells lose many excitatory synapses by 5 days after status epilepticus, which are replaced later in epileptic rats close to normal levels.

To more precisely determine where changes occurred, numbers of GABA-negative synapses per granule cell were evaluated by strata (Fig. 6E). The average number of GABA-negative synapses per granule cell in controls was 2,730 ± 250 in the inner molecular layer and 8,040 ± 820 in the outer molecular layer. In the inner molecular layer, the average number of GABA-negative synapses per granule cell at 5 days after status epilepticus was reduced to 1,050 ± 50 (38% of controls) and later recovered to 2,300 ± 220 (84% of controls) in epileptic rats. In the outer molecular layer, the average number of GABA-negative synapses per granule cell at 5 days after status epilepticus was reduced to 5,530 ± 150 (69% of controls) and later recovered to 8,120 ± 690 (101% of controls) in epileptic rats. These findings suggest glutamatergic synapse loss and later recovery occurs throughout the molecular layer but is relatively more severe in the inner third.

In the molecular layer, glutamatergic synapses are found with dendritic spines and shafts. In control rats, 230 ± 45 GABA-negative synapses per granule cell were with dendritic shafts, and 10,540 ± 1,000 (98% of control) were with spines (Fig. 6F). Previous studies found similar high proportions of axo-spinous GABA-negative synapses in the molecular layer (Matthews et al., 1976). Shaft synapses were twice as numerous at 5 days after status epilepticus (449 ± 99) and in epileptic rats (466 ± 58) compared to controls. The average number of axo-spinous synapses at 5 days after status epilepticus was 6,130 ± 90 (58% of control levels) ($P < 0.05$, ANOVA, Student–Newman–Keuls method) and recovered to 9,950 ± 760 (94% of controls) in epileptic rats.

Previous studies suggest that larger glutamatergic synapses might be more effective, in part, because they might have more readily releasable vesicles (Murthy et al., 2001) and more postsynaptic receptors (Nusser et al., 1998). In the inner and outer molecular layer, average areas of GABA-negative postsynaptic densities were 0.046 ± 0.001 μm^2 and 0.041 ± 0.002 μm^2 in controls, respectively (Fig. 6G), similar to previous reports (Trommald and Hulleberg, 1997). In the outer molecular layer there was a progressive trend toward larger synapse areas in rats 5 days after status epilepticus (0.048 ± 0.002 μm^2) and epileptic animals (0.050 ± 0.004 μm^2), which were 115% and 120% of controls, respectively. In the inner molecular layer, average GABA-negative synapse area was similar in controls (0.046

± 0.001 μm^2) and rats 5 days after status epilepticus (0.045 ± 0.001 μm^2). In epileptic rats, on the other hand, GABA-negative synapse area in the inner molecular increased to 0.060 ± 0.004 μm^2 (132% of controls) ($P < 0.05$, ANOVA, Student–Newman–Keuls method).

Most GABA-negative synapses had a postsynaptic density consisting of a simple, complete disc. At larger synapses, however, postsynaptic densities sometimes were perforated, as described previously (Peters et al., 1991). Previous studies suggest perforated synapses might express high levels of glutamate receptors (Ganeshina et al., 2004). Perforated synapses have been reported to occur at 7% of synapses in the molecular layer of control rats (Curcio and Hinds, 1983). In the present study, in the outer molecular layer 8.0 ± 1.9% of GABA-negative synapses were perforated in controls (Fig. 6H). There was a trend toward larger proportions of perforated synapses in rats 5 days after status epilepticus (10.3 ± 2.7%) and epileptic animals (10.9 ± 0.7%), which were 1.3 and 1.4 times control levels, respectively. In the inner molecular layer, 7.6 ± 0.8% of GABA-negative synapses were perforated in controls. In rats 5 days after status epilepticus, the average proportion of perforated synapses in the inner molecular layer was reduced almost by half (4.0 ± 1.6%). In epileptic rats, on the other hand, the average proportion of perforated synapses in the inner molecular was 16.2 ± 2.7%, more than twice control levels ($P < 0.05$, ANOVA, Student–Newman–Keuls method). Together, these findings reveal that excitatory synapses in the inner molecular of epileptic rats were larger and more likely to be perforated.

DISCUSSION

The principal findings of this study include the following. Numbers of gephyrin-immunoreactive punctae per dentate gyrus, numbers of EM identified GABAergic synapses per dentate gyrus, and numbers of GABAergic synapses per granule cell were reduced in pilocarpine-treated rats 5 days after status epilepticus but increased later beyond control levels in epileptic rats. Most GABAergic synapse loss and later proliferation occurred in the outer molecular layer. Axo-spinous synapses accounted for most of the GABAergic synapse loss, whereas axo-spinous and axo-shaft synapses accounted for most of the GABAergic synapse gain. Excitatory synapses per granule cell also were reduced 5 days after status epilepticus and recovered almost to control levels in epileptic animals. In epileptic rats, excitatory synapses in the inner molecular layer were more likely to be perforated synapses and were larger than in controls.

Estimating synapse numbers

We used an optical fractionator method and large series of consecutive electron micrographs to estimate excitatory and inhibitory synapse numbers in the dentate gyrus of a rat model of temporal lobe epilepsy. Our estimate of excitatory synapses per dentate gyrus molecular layer of control rats (13.86×10^9) is similar to that of a study that used a physical dissector method (13.85×10^9) (Cardoso et al., 2008). Inhibitory synapses are more challenging to identify (Gray, 1959), so two methods were used in the present study: gephyrin-immunoreactivity and EM with postembedding GABA immunocytochemistry. Postembedding immunocytochemistry detects low levels of GABA in control granule cell axons, but not in their somata or dendrites (Sandler and Smith, 1991). Seizure activity increases GABA expression by granule cells (Sloviter et al., 1996b), raising the possibility that GABA-positive profiles in the present study might have been incorrectly identified as interneurons instead of granule cells. For axons, this seems unlikely, because ultrastructurally almost all of the synapses formed by GABA-positive axons were symmetric, not asymmetric like synapses formed by the axons of glutamatergic neurons including granule cells. For somata and dendrites, this seems even more unlikely, because the vast majority of cell body and dendritic profiles in the granule cell layer and dendritic profiles in the inner molecular layer were GABA-negative. GABA-positive profiles were

evident but relatively rare and isolated, as expected for interneurons and unlike the very common GABA-negative presumed granule cell profiles.

Our estimates of GABAergic synapse numbers are higher than previous reports for control rats. One study used immunoreactivity for GAD67 to identify GABAergic axon terminals in the granule cell layer and estimated 2.43×10^8 synapses (Shi et al., 2004), which is two-thirds our value. The difference might be attributable to incomplete labeling of GABAergic synapses with GAD67 immunocytochemistry (Esclapez and Houser, 1999). Another study used EM with postembedding GABA immunocytochemistry to estimate 1.90×10^9 GABAergic synapses per granule cell layer plus molecular layer (Halasy and Somogyi, 1993a), which is one-third our estimate. That study did not analyze serial sections and made assumptions about shrinkage and volumes. The stereological approach used in the present study, which is based on Geinesman et al. (1996, 2000), measures volumes of analyzed regions directly and avoids assumptions about shrinkage.

Combining our excitatory and inhibitory synapse data suggests that 28% of all synapses with granule cells in control rats are GABAergic. This value is higher than that reported for neurons in various neocortical areas and species (DeFelipe et al., 2002). It also is higher than previous reports for granule cells (Crain et al., 1973; Matthews et al., 1976; Nadler et al., 1980a), but those studies did not use postembedding GABA immunoreactivity, which detects asymmetric inhibitory synapses, nor did they analyze serial sections, which facilitates inhibitory synapse identification. Previously we used postembedding GABA immunocytochemistry and serial EM and found that 8% of synapses with basal dendrites are GABAergic (Thind et al., 2008). These findings, compared with results from the present study for granule cell apical dendrites, suggest granule cell basal dendrites, which develop after epileptogenic injuries, are relatively less inhibited than apical dendrites. In the present study, granule cell basal dendrites were not evaluated, because they are located in the hilus, where they intermingle with dendrites of other neuronal types (for example, surviving mossy cells) that would be difficult to distinguish from granule cell basal dendrites with the EM stereological approach used.

Short-term loss of GABAergic synapses

At 5 days after status epilepticus, numbers of GAD-positive interneurons per dentate gyrus, numbers of gephyrin-immunoreactive punctae per dentate gyrus, and numbers of GABAergic synapses per granule cell all were reduced to ≤71% of control levels. Some GABAergic axons project into dentate gyrus from other regions, but they are rare (Germroth et al., 1989) or preferentially target interneurons not granule cells (Freund and Antal, 1988). Therefore, most GABAergic synapse loss is likely attributable to loss of interneurons within the dentate gyrus. Substantial loss of somatostatin-immunoreactive interneurons occurs in patients with temporal lobe epilepsy (de Lanerolle et al., 1989; Mathern et al., 1995; Sundstrom et al., 2001) and rodent models (Sloviter, 1987; Freund et al., 1991; Lowenstein et al., 1992; Schwarzer et al., 1995; Houser and Esclapez, 1996; Buckmaster and Jongen-Rêlo, 1999; Sun et al., 2007). Somatostatin interneurons are GABAergic (Somogyi et al., 1984; Kosaka et al., 1988; Esclapez and Houser, 1995) and account for 25% of all GABAergic neurons within the dentate gyrus (Austin and Buckmaster, 2004). Their axon collaterals extend across broad septotemporal spans of hippocampus (Boyett and Buckmaster, 2001; Buckmaster et al., 2002a), concentrate in the outer molecular layer (Bakst et al., 1996), and synapse with dendritic shafts and spines of granule cells (Milner and Bacon, 1989; Leranth et al., 1990; Katona et al., 1999a). The present study revealed that at 5 days after status epilepticus, most GABAergic synapse loss occurred with spines in the outer molecular layer. Previous studies showed that hippocampal GAD activity is reduced (Turski et al., 1986) and the outer molecular layer displays lower densities of GAD-immunoreactive punctae (Houser and Esclapez, 1996) 5–7 days after pilocarpine-induced

status epilepticus. Loss of GABAergic synapses, especially in the outer molecular layer, might account, at least in part, for hyperexcitable responses to perforant path stimulation (Sloviter, 1992; Wasterlain et al., 1996; Hellier et al., 1999; Ang et al., 2006) and reduced frequencies of mIPSCs in granule cells shortly after status epilepticus (Kobayashi and Buckmaster, 2003; Shao and Dudek, 2005; Sun et al., 2007). Video-EEG seizure monitoring reveals that in chemoconvulsant models of temporal lobe epilepsy, rats sometimes begin displaying spontaneous seizures within 1–2 weeks after status epilepticus (Goffin et al., 2007; Jung et al., 2007; Williams et al., 2009). Acute loss of GABAergic synapses with granule cells might contribute to lowered seizure threshold at that timepoint.

GABAergic synaptogenesis

In response to pathophysiological conditions, GABAergic interneurons in adult animals appear to sprout axons and form new synapses. For example, weeks after lesioning perforant path input to the dentate gyrus, GAD activity (Nadler et al., 1974) and immunoreactivity (Goldowitz et al., 1982) increase in the outer molecular layer, gephyrin punctae increase in the molecular layer (Simbürger et al., 2000, 2001), and GABAergic axons labeled with antero-grade tracer sprout in the outer molecular layer (Deller et al., 1995). In mouse models of Alzheimer's disease, immunoreactive markers of GABAergic axons, including somatostatin, increase in the dentate gyrus (Palop et al., 2007). Similarly, the dentate gyrus of patients and rodent models of temporal lobe epilepsy displays increased expression of markers of GABAergic axons (see Introduction) and synapses (Schwarzer et al., 1997; Fritschy et al., 1999; Knuesel et al., 2001). However, it is difficult to distinguish genuine axon sprouting and synaptogenesis from increased marker expression by preexisting structures (Bausch, 2005). Limited EM data are consistent with GABAergic synaptogenesis in the epileptic dentate gyrus (Wittner et al., 2001), and light microscopic data are supportive (Arellano et al., 2004).

In the present study, epileptic rats had 1.8 times more gephyrin-immunoreactive punctae per dentate gyrus and twice as many GABAergic synapses per granule cell as rats 5 days after status epilepticus, while numbers of GABAergic interneurons per dentate gyrus were similar, suggesting surviving interneurons made new GABAergic synapses with granule cells. Previously it was reported that GABA levels in the hippocampus increase to 172% of controls in epileptic rats (Cavalheiro et al., 1994). Together, these data suggest that surviving interneurons sprout axons and develop new synapses with granule cells. Underlying mechanisms of epilepsy-related interneuron axon sprouting are unclear, but brain-derived neurotrophic factor is upregulated by seizures (Isackson et al., 1991) and promotes GABAergic synaptogenesis (Vicario-Abejón et al., 1998).

Most new GABAergic synapses developed in the outer molecular layer with shafts and spines of granule cell dendrites, suggesting somatostatin interneurons are a likely source. However, other interneurons within and outside of the dentate gyrus might contribute. In the inner molecular layer, numbers of GABAergic synapses increased but less than in the outer molecular of epileptic rats. In contrast, previous studies found that immunocytochemical markers of GABAergic axons and synapses increase more in the inner than the outer molecular layer (de Lanerolle et al., 1989; Davenport et al., 1990; Mathern et al., 1995, 1997, 1999; Houser and Esclapez, 1996; Bausch and Chavkin, 1997; Esclapez and Houser, 1999; André et al., 2001; Boulland et al., 2007). Causes of this difference are unclear but might include indirect versus direct measures of GABAergic synapses.

Functional consequences of GABAergic synaptogenesis might include restoration of inhibition lost when vulnerable interneurons died, which is consistent with normal or enhanced measures of granule cell inhibition sometimes found in epileptic tissue (Haas et al., 1996; Isokawa, 1996; Bausch and Chavkin, 1997; Buckmaster and Dudek, 1999;

Okazaki et al., 1999). However, granule cell mIPSC frequency, which depends primarily on GABAergic synapse number and synaptic release probability, remains low in epileptic rats (Kobayashi and Buckmaster, 2003; Shao and Dudek, 2005; Sun et al., 2007; but see Leroy et al., 2004). A mechanism that could contribute to less frequent mIPSCs in granule cells, despite abundant GABAergic synapses, is reduced probability of GABA release. In support, unitary IPSCs at basket cell-to-granule cell synapses are significantly more likely to fail in epileptic rats compared with controls (Zhang and Buckmaster, 2009). It is unclear whether synaptic efficacy to granule cells from other dentate interneurons is reduced. In a rat model of temporal lobe epilepsy, mIPSCs are less frequent in CA1 pyramidal cells, and densities of synaptic vesicles are reduced in GABAergic synapses with pyramidal cell bodies, which was attributed to reduced reserve pools of synaptic vesicles (Hirsch et al., 1999). Some basket cell synapses with CA1 pyramidal cells are CCK-immunoreactive and express cannabinoid receptors (Katona et al., 1999b; Tsou et al., 1999). At those synapses, GABAergic transmission is modulated by cannabinoid receptor activation (Glickfeld and Scanziani, 2006), and cannabinoid-dependent presynaptic inhibition of GABA release increases long-term after febrile seizures (Chen et al., 2003), which are common in patients who later develop temporal lobe epilepsy. Together, these findings suggest epileptic tissue may contain abundant but dysfunctional synapses. If so, restoring proper function of newly formed GABAergic synapses in epileptic tissue might be anticonvulsant. On the other hand, excessive GABAergic synapses have been proposed as hypersynchronizing and proconvulsant (Babb et al., 1989). Excessive GABAergic receptor activation can depolarize, especially dendrites (Staley et al., 1995) where proliferation of GABAergic synapses was most severe in epileptic animals. Thus, at this time, functional consequences of GABAergic synaptogenesis in epileptic tissue remain unclear.

Excitatory synapses

Previously it was shown that intraventricular kainate causes loss of excitatory synapses in the dentate molecular layer, which eventually recover to near normal levels (Nadler et al., 1980b). Results of the present study are similar. At 5 days after status epilepticus, substantial loss of excitatory synapses in the inner molecular layer is likely attributable to loss of hilar mossy cells (Buckmaster and Jongen-Rêlo, 1999; Jiao and Nadler, 2007; Boulland et al., 2007), which project axons to this area (Berger et al., 1980; Buckmaster et al., 1996). In the present study, the extent of excitatory synapse loss in the outer molecular layer short-term (reduced to 69% of control levels) is similar to the extent of reductions in immunoreactivity for synaptophysin 5 days after kainate-induced seizures (Yuan et al., 2002) and reductions in numbers of layer II entorhinal cortical neurons in epileptic pilocarpine-treated rats (Kumar and Buckmaster, 2006). These findings suggest that status epilepticus substantially reduces perforant path input to granule cells. Loss of excitatory synapses with granule cells might transiently shift input– output curves of perforant path stimulation as has been reported shortly after status epilepticus (Gorter et al., 2002).

In epileptic rats, numbers of excitatory synapses in the outer molecular layer returned to control levels, suggesting sprouting and synaptogenesis by surviving layer II entorhinal cortical neurons. If fewer layer II entorhinal cortical neurons together form the same number of excitatory synapses with the same number of granule cells, then individual entorhinal cortical neurons in epileptic rats might innervate more granule cells, which might have synchronizing effects. In the inner molecular layer, excitatory synapse numbers per granule cell returned to 84% of control levels. Ultrastructural evidence shows that glutamatergic synapses in the inner molecular layer of patients with temporal lobe epilepsy and rodent models arise, at least in part, from granule cell axons (Sutula et al., 1989; Babb et al., 1991; Represa et al., 1993; Franck et al., 1995; Okazaki et al., 1995; Zhang and Houser, 1999; Wenzel et al., 2000; Buckmaster et al., 2002b). However, other sources might contribute,

including supramammillary nucleus (Maglóczky et al., 1994) and surviving mossy cells. In epileptic rats, excitatory synapses in the inner molecular layer were larger, and more were perforated, suggesting excitatory synapses in epileptic animals might be stronger, consistent with recordings obtained from granule cells in epileptic animals (Wuarin and Dudek, 2001; Scimemi et al., 2006).

In summary, shortly after status epilepticus, numbers of inhibitory and excitatory synapses to granule cells are substantially reduced, probably because of excitotoxic death of presynaptic neurons. Over time, excitatory synapse numbers return approximately to normal levels, and excitatory synapses in the inner molecular layer enlarge. Inhibitory synapse numbers eventually overshoot control levels, especially in the outer molecular layer. These findings reveal remarkable plasticity of excitatory and inhibitory circuits in an adult brain after an epileptogenic injury.

Acknowledgments

We thank Dr. Lisa Hsuan for assistance developing a gephyrin stereology protocol.

Grant sponsors: National Institute of Neurological Disorders and Stroke (NINDS) and National Center for Research Resources (NCRR) of the National Institutes of Health (NIH).

LITERATURE CITED

André V, Marescaux C, Nehlig A, Fritschy JM. Alterations of hippocampal GABAergic system contribute to development of spontaneous recurrent seizures in the rat lithium-pilocarpine model of temporal lobe epilepsy. Hippocampus. 2001; 11:452–468. [PubMed: 11530850]

Andrioli A, Alonso-Nanclares L, Arellano JI, DeFelipe J. Quantitative analysis of parvalbumin-immunoreactive cells in the human epileptic hippocampus. Neuroscience. 2007; 149:131–143. [PubMed: 17850980]

Ang CW, Carlson GC, Coulter DA. Massive and specific dysregulation of direct cortical input to the hippocampus in temporal lobe epilepsy. J Neurosci. 2006; 26:11850–11856. [PubMed: 17108158]

Arellano JI, Muñoz A, Ballesteros-Yáñnez I, Sola RG, DeFelipe J. Histopathology and reorganization of chandelier cells in the human epileptic sclerotic hippocampus. Brain. 2004; 127:45–64. [PubMed: 14534159]

Austin JE, Buckmaster PS. Recurrent excitation of granule cells with basal dendrites and low interneuron density and inhibitory postsynaptic current frequency in the dentate gyrus of macaque monkeys. J Comp Neurol. 2004; 476:205–218. [PubMed: 15269966]

Babb TL, Pretorius JK, Kupfer WR, Crandall PH. Glutamate decarboxylase-immunoreactive neurons are preserved in human epileptic hippocampus. J Neurosci. 1989; 9:2562–2574. [PubMed: 2501460]

Babb TL, Kupfer WR, Pretorius JK, Crandall PH, Levesque MF. Synaptic reorganization by mossy fibers in human epileptic fascia dentata. Neuroscience. 1991; 42:351–363. [PubMed: 1716744]

Bakst I, Avendano C, Morrison JH, Amaral DG. An experimental analysis of the origins of somatostatin-like immunoreactivity in the dentate gyrus of the rat. J Neurosci. 1986; 6:1452–1462. [PubMed: 2872280]

Bausch SB. Axonal sprouting of GABAergic interneurons in temporal lobe epilepsy. Epilepsy Behav. 2005; 7:390–400. [PubMed: 16198153]

Bausch SB, Chavkin C. Changes in hippocampal circuitry after pilocarpine-induced seizures as revealed by opioid receptor distribution and activation. J Neurosci. 1997; 17:477–492. [PubMed: 8987772]

Berger TW, Semple-Rowland S, Basset JL. Hippocampal polymorph neurons are the cells of origin for ipsilateral association and commissural afferents to the dentate gyrus. Brain Res. 1980; 215:329–336. [PubMed: 6167320]

Boulland J-L, Ferhat L, Solbu TT, Ferrand N, Chaudhry FA, Storm-Mathisen J, Esclapez M. Changes in vesicular transporters for γ-aminobutyric acid and glutamate reveal vulnerability and reorganization of hippocampal neurons following pilocarpine-induced seizures. J Comp Neurol. 2007; 503:466–485. [PubMed: 17503488]

Boyett JM, Buckmaster PS. Somatostatin-immunoreactive interneurons contribute to lateral inhibitory circuits in the dentate gyrus of control and epileptic rats. Hippocampus. 2001; 11:418–422. [PubMed: 11530846]

Buckmaster PS. Laboratory animal models of temporal lobe epilepsy. Comp Med. 2004; 54:473–485. [PubMed: 15575361]

Buckmaster PS, Dudek FE. Neuron loss, granule cell axon reorganization, and functional changes in the dentate gyrus of epileptic kainate-treated rats. J Comp Neurol. 1997; 385:385–404. [PubMed: 9300766]

Buckmaster PS, Dudek FE. In vivo intracellular analysis of granule cell axon reorganization in epileptic rats. J Neurophysiol. 1999; 81:712–721. [PubMed: 10036272]

Buckmaster PS, Jongen-Rélo AL. Highly specific neuron loss preserves lateral inhibitory circuits in the dentate gyrus of kainate-induced epileptic rats. J Neurosci. 1999; 19:9519–9529. [PubMed: 10531454]

Buckmaster PS, Strowbridge BW, Kunkel DD, Schmiege DL, Schwartzkroin PA. Mossy cell axonal projections to the dentate gyrus molecular layer in the rat hippocampal slice. Hippocampus. 1992; 2:349–362. [PubMed: 1284975]

Buckmaster PS, Wenzel HJ, Kunkel DD, Schwartzkroin PA. Axon arbors and synaptic connections of hippocampal mossy cells in the rat in vivo. J Comp Neurol. 1996; 366:270–292.

Buckmaster PS, Yamawaki R, Zhang GF. Axon arbors and synaptic connections of a vulnerable population of interneurons in the dentate gyrus in vivo. J Comp Neurol. 2002a; 445:360–373. [PubMed: 11920713]

Buckmaster PS, Zhang GF, Yamawaki R. Axon sprouting in a model of temporal lobe epilepsy creates a predominantly excitatory feedback circuit. J Neurosci. 2002b; 22:6650–6658. [PubMed: 12151544]

Cardoso A, Assunção, Andrade JP, Pereira PA, Madeira MD, Paula-Barbosa MM, Lukoyanov NV. Loss of synapses in the entorhinal-dentate gyrus pathway following repeated induction of electroshock seizures in the rat. J Neurosci Res. 2008; 86:71–83. [PubMed: 17705293]

Cavalheiro EA, Fernandes MJ, Turski L, Naffah-Mazzacoratti MG. Spontaneous recurrent seizures in rats: amino acid and monoamine determination in the hippocampus. Epilepsia. 1994; 35:1–11. [PubMed: 8112229]

Chen K, Ratzliff A, Hilgenberg L, Gulyás A, Freund TF, Smith M, Dinh TP, Piomelli D, Mackie K, Soltesz I. Long-term plasticity of endocannabinoid signaling induced by developmental febrile seizures. Neuron. 2003; 39:599–611. [PubMed: 12925275]

Craig AM, Banker G, Chang W, McGrath ME, Serpinskaya AS. Clustering of gephyrin at GABAergic but not glutamatergic synapses in cultured rat hippocampal neurons. J Neurosci. 1996; 16:3166–3177. [PubMed: 8627355]

Crain B, Cotman C, Taylor D, Lynch G. A quantitative electron microscopic study of synaptogenesis in the dentate gyrus of the rat. Brain Res. 1973; 63:195–204. [PubMed: 4764297]

Curcio CA, Hinds JW. Stability of synaptic density and spine volume in dentate gyrus of aged rats. Neurobiol Aging. 1983; 4:77–87. [PubMed: 6877491]

Davenport CJ, Brown WJ, Babb TL. Sprouting of GABAergic and mossy fiber axons in dentate gyrus following intrahippocampal kainate in the rat. Exp Neurol. 1990; 109:180–190. [PubMed: 1696207]

de Lanerolle NC, Kim JH, Robbins RJ, Spencer DD. Hippocampal interneuron loss and plasticity in human temporal lobe epilepsy. Brain Res. 1989; 495:387–395. [PubMed: 2569920]

DeFelipe J, Alonso-Nanclares L, Arellano JI. Microstructure of the neocortex: comparative aspects. J Neurocytol. 2002; 31:299–316. [PubMed: 12815249]

Deller T, Frotscher M, Nitsch R. Morphological evidence for the sprouting of inhibitory commissural fibers in response to the lesion of the excitatory entorhinal input to the rat dentate gyrus. J Neurosci. 1995; 15:6868–6878. [PubMed: 7472444]

Engel, J., Jr; Williamson, PD.; Wieser, H-G. Mesial temporal lobe epilepsy. In: Engel, J., Jr; Pedley, TA., editors. Epilepsy: a comprehensive textbook. Lippincott-Raven; Philadelphia: 1997. p. 2417-2426.

Erlander MG, Tillakaratne NJK, Feldblum S, Patel N, Tobin AJ. Two genes encode distinct glutamate decarboxylases. Neuron. 1991; 7:91–100. [PubMed: 2069816]

Esclapez M, Houser CR. Somatostatin neurons are a sub-population of GABA neurons in the rat dentate gyrus: evidence from colocalization of pre-prosomatostatin and glutamate decarboxylase messenger RNAs. Neuroscience. 1995; 64:339–355. [PubMed: 7700525]

Esclapez M, Houser CR. Up-regulation of GAD65 and GAD67 in remaining hippocampal GABA neurons in a model of temporal lobe epilepsy. J Comp Neurol. 1999; 412:488–505. [PubMed: 10441235]

Fifková E, Eason H, Schaner P. Inhibitory contacts on dendritic spines of the dentate fascia. Brain Res. 1992; 577:331–336. [PubMed: 1606504]

Franck JE, Pokorny J, Kunkel DD, Schwartzkroin PA. Physiologic and morphologic characteristics of granule cell circuitry in human epileptic hippocampus. Epilepsia. 1995; 36:543–558. [PubMed: 7555966]

Freund TF, Antal M. GABA-containing neurons in the septum control inhibitory interneurons in the hippocampus. Nature. 1988; 336:170–173. [PubMed: 3185735]

Freund TF, Ylinen A, Miettinen R, Pitkänen, Lahtinen H, Baimbridge KG, Riekkinen PJ. Pattern of neuronal death in the rat hippocampus after status epilepticus. Relationship to calcium binding protein content and ischemic vulnerability. Brain Res Bull. 1991; 28:27–38. [PubMed: 1347249]

Fritschy J-M, Kiener T, Bouilleret V, Loup F. GABAergic neurons and $GABA_A$-receptors in temporal lobe epilepsy. Neurochem Int. 1999; 34:435–445. [PubMed: 10397372]

Ganeshina O, Berry RW, Petralia RS, Nicholson DA, Geinesman Y. Differences in the expression of AMPA and NMDA receptors between axospinous perforated and nonperforated synapses are related to the configuration and size of postsynaptic densities. J Comp Neurol. 2004; 468:86–95. [PubMed: 14648692]

Geinesman Y, Gundersen HJG, Van der Zee E, West MJ. Unbiased stereological estimation of the total number of synapses in a brain region. J Neurocytol. 1996; 25:805–819. [PubMed: 9023726]

Geinesman Y, Disterhoft JF, Gundersen HJG, McEchron MD, Persina IS, Power JM, Van der Zee EA, West MJ. Remodeling of hippocampal synapses after hippocampus-dependent associative learning. J Comp Neurol. 2000; 417:49–59. [PubMed: 10660887]

Germroth P, Schwerdtfeger WK, Buhl EH. GABAergic neurons in the entorhinal cortex project to the hippocampus. Brain Res. 1989; 494:187–192. [PubMed: 2765919]

Glickfeld LL, Scanziani M. Distinct timing in the activity of cannabinoid-sensitive and cannabinoid-insensitive basket cells. Nat Neurosci. 2006; 9:807–815. [PubMed: 16648849]

Goffin K, Nissinen J, Van Laere K, Pitkänen A. Cyclicity of spontaneous recurrent seizures in pilocarpine model of temporal lobe epilepsy in rat. Exp Neurol. 2007; 205:501–505. [PubMed: 17442304]

Goldowitz D, Vincent SR, Wu J-Y, Hökfelt T. Immunohistochemical demonstration of plasticity in GABA neurons of the adult rat dentate gyrus. Brain Res. 1982; 238:413–420. [PubMed: 7046874]

Gorter JA, van Vliet EA, Aronica E, Lopes da Silva FH. Progression of spontaneous seizures after status epilepticus is associated with mossy fibre sprouting and extensive bilateral loss of hilar parvalbumin and somatostatin-immunoreactive neurons. Eur J Neurosci. 2001; 13:657–669. [PubMed: 11207801]

Gorter JA, van Vliet EA, Aronica E, Lopes da Silva FH. Long-lasting increased excitability differs in dentate gyrus vs. CA1 in freely moving chronic epileptic rats after electrically induced status epilepticus. Hippocampus. 2002; 12:311–324. [PubMed: 12099483]

Gray EG. Axo-somatic and axo-dendritic synapses of the cerebral cortex. J Anat (Lond). 1959; 93:420–433. [PubMed: 13829103]

Haas KZ, Sperber EF, Moshé SL, Stanton PK. Kainic acid-induced seizures enhance dentate gyrus inhibition by down-regulation of $GABA_B$ receptors. J Neurosci. 1996; 16:4250–4260. [PubMed: 8753886]

Halasy K, Somogyi P. Distribution of GABAergic synapses and their targets in the dentate gyrus of rat: a quantitative immunoelectron microscopic analysis. J Hirnforsch. 1993a; 34:299–308. [PubMed: 8270784]

Halasy K, Somogyi P. Subdivisions in the multiple GABAergic innervation of granule cells in the dentate gyrus of the rat hippocampus. Eur J Neurosci. 1993b; 5:411–429. [PubMed: 8261118]

Han Z-S, Buhl EH, Lörinczi Z, Somogyi P. A high degree of spatial selectivity in the axonal and dendritic domains of physiologically identified local-circuit neurons in the dentate gyrus of the rat hippocampus. Eur J Neurosci. 1993; 5:395–410. [PubMed: 8261117]

Hellier JL, Patrylo PR, Dou P, Nett M, Rose GM, Dudek FE. Assessment of inhibition and epileptiform activity in the septal dentate gyrus of freely behaving rats during the first week after kainate treatment. J Neurosci. 1999; 19:10053–10064. [PubMed: 10559413]

Hirsch JC, Agassandian C, Merchán-Pérez A, Ben-Ari Y, DeFilipe J, Esclapez M, Bernard C. Deficit of quantal release of GABA in experimental models of temporal lobe epilepsy. Nat Neurosci. 1999; 2:499–500. [PubMed: 10448211]

Houser CR, Esclapez M. Vulnerability and plasticity of the GABA system in the pilocarpine model of spontaneous recurrent seizures. Epilepsy Res. 1996; 26:207–218. [PubMed: 8985701]

Isackson PJ, Huntsman MM, Murray KD, Gall CM. BDNF mRNA expression is increased in adult rat forebrain after limbic seizures: temporal patterns of induction distinct from NGF. Neuron. 1991; 6:937–948. [PubMed: 2054188]

Isokawa M. Decrement of $GABA_A$ receptor-mediated inhibitory postsynaptic currents in dentate granule cells in epileptic hippocampus. J Neurophysiol. 1996; 75:1901–1908. [PubMed: 8734589]

Jiao Y, Nadler JV. Stereological analysis of GluR2-immunoreactive hilar neurons in the pilocarpine model of temporal lobe epilepsy: correlation of cell loss with mossy fiber sprouting. 2007; 205:569–582.

Jung S, Jones TD, Lugo JN Jr, Sheerin AH, Miller JW, D'Ambrosio R, Anderson AE, Poolos NP. Progressive dendritic HCN channelopathy during epileptogenesis in the rat pilocarpine model of epilepsy. J Neurosci. 2007; 27:13012–13021. [PubMed: 18032674]

Katona I, Acsády L, Freund TF. Postsynaptic targets of somatostatin-immunoreactive interneurons in the rat hippocampus. Neuroscience. 1999a; 88:37–55. [PubMed: 10051188]

Katona I, Sperlágh B, Sík A, Käfalvi A, Vizi ES, Mackie K, Freund TF. Presynaptically located CB1 cannabinoid receptors regulate GABA release from axon terminals of specific hippocampal interneurons. J Neurosci. 1999b; 19:4544–4558. [PubMed: 10341254]

Kirsch J, Betz H. Widespread expression of gephyrin, a putative glycine receptor-tubulin linker protein, in rat brain. Brain Res. 1993; 631:301–310. [PubMed: 8242343]

Knuesel I, Zuellig RA, Schaub MC, Fritschy J-M. Alterations in dystrophin and utrophin expression parallel the reorganization of GABAergic synapses in a mouse model of temporal lobe epilepsy. Eur J Neurosci. 2001; 13:1113–1124. [PubMed: 11285009]

Kobayashi M, Buckmaster PS. Reduced inhibition of dentate granule cells in a model of temporal lobe epilepsy. J Neurosci. 2003; 23:2440–2452. [PubMed: 12657704]

Kosaka T, Hama K, Wu J-Y. GABAergic synaptic boutons in the granule cell layer of the rat dentate gyrus. Brain Res. 1984; 293:353–359. [PubMed: 6320972]

Kosaka T, Wu J-Y, Benoit R. GABAergic neurons containing somatostatin-like immunoreactivity in the rat hippocampus and dentate gyrus. Exp Brain Res. 1988; 71:388–398. [PubMed: 3169171]

Kumar SS, Buckmaster PS. Hyperexcitability, interneurons, and loss of GABAergic synapses in entorhinal cortex in a model of temporal lobe epilepsy. J Neurosci. 2006; 26:4613–4623. [PubMed: 16641241]

Leranth C, Malcolm AJ, Frotscher M. Afferent and efferent synaptic connections of somatostatin-immunoreactive neurons in the rat fascia dentata. J Comp Neurol. 1990; 295:111–122. [PubMed: 1971287]

Leroy C, Poisbeau P, Keller AF, Nehlig A. Pharmacological plasticity of $GABA_A$ receptors at dentate gyrus synapses in a rat model of temporal lobe epilepsy. J Physiol (Lond). 2004; 557:473–487. [PubMed: 15034126]

Lowenstein DH, Thomas MJ, Smith DH, McIntosh TK. Selective vulnerability of dentate hilar neurons following traumatic brain injury: a potential mechanistic link between head trauma and disorders of the hippocampus. J Neurosci. 1992; 12:4846–4853. [PubMed: 1464770]

Maglóczky, Zs; Acsády, L.; Freund, TF. Principal cells are the postsynaptic targets of supramammillary afferents in the hippocampus of the rat. Hippocampus. 1994; 4:322–334. [PubMed: 7531093]

Maglóczky, Zs; Wittner, L.; Borhegyi, Zs; Halász, P.; Vajda, J.; Freund, TF. Changes in the distribution and connectivity of interneurons in the epileptic human dentate gyrus. Neuroscience. 2000; 96:7–25. [PubMed: 10683405]

Margerison HJ, Corsellis JAN. Epilepsy and the temporal lobes. Brain. 1966; 89:499–530. [PubMed: 5922048]

Mathern GW, Babb TL, Pretorius JK, Leite JP. Reactive synaptogenesis and neuron densities for neuropeptide Y, somatostatin, and glutamate decarboxylase immunoreactivity in the epileptogenic human fascia dentata. J Neurosci. 1995; 15:3990–4004. [PubMed: 7751960]

Mathern GW, Bertram EH, Babb TL, Pretorius JK, Kuhlman PA, Spradlin S, Mendoza D. In contrast to kindled seizures, the frequency of spontaneous epilepsy in the limbic status model correlates with greater aberrant fascia dentata excitatory and inhibitory axon sprouting, and increased staining for N-methyl-D-aspartate, AMPA, and $GABA_A$ receptors. Neuroscience. 1997; 77:1003–1019. [PubMed: 9130782]

Mathern GW, Mendoza D, Lozada A, Pretorius JK, Dehnes Y, Danbolt NC, Nelson N, Leite JP, Chimelli L, Born DE, Sakamoto AC, Assirati JA, Fried I, Peacock WJ, Ojemann GA, Adelson PD. Hippocampal GABA and glutamate transporter immunoreactivity in patients with temporal lobe epilepsy. Neurology. 1999; 52:453–472. [PubMed: 10025773]

Matthews DA, Cotman C, Lynch G. An electron microscopic study of lesion-induced synaptogenesis in the dentate gyrus of the adult rat. I. Magnitude and time course of degeneration. Brain Res. 1976; 115:1–21. [PubMed: 974734]

McCloskey DP, Hintz TM, Pierce JP, Scharfman HE. Stereological methods reveal the robust size and stability of ectopic hilar granule cells after pilocarpine-induced status epilepticus in the adult rat. Eur J Neurosci. 2006; 24:2203–2210. [PubMed: 17042797]

Miles R, Tóth K, Gulyás AI, Hájos N, Freund T. Differences between somatic and dendritic inhibition in the hippocampus. Neuron. 1996; 16:815–823. [PubMed: 8607999]

Milner TA, Bacon CE. Ultrastructural localization of somatostatin-like immunoreactivity in the rat dentate gyrus. J Comp Neurol. 1989; 290:544–560. [PubMed: 2613944]

Murthy VN, Schikorski T, Stevens CF, Zhu Y. Inactivity produces increases in neurotransmitter release and synapse size. Neuron. 2001; 32:673–682. [PubMed: 11719207]

Nadler JV, Cotman CW, Lynch GS. Biochemical plasticity of short-axon interneurons: increased glutamate decarboxylase activity in the denervated area of rat dentate gyrus following entorhinal lesion. Exp Neurol. 1974; 45:403–413. [PubMed: 4153783]

Nadler JV, Perry BW, Gentry C, Cotman CW. Loss and reacquisition of hippocampal synapses after selective destruction of CA3-CA4 afferents with kainic acid. Brain Res. 1980a; 191:387–403. [PubMed: 7378766]

Nadler JV, Perry BW, Cotman CW. Selective reinnervation of hippocampal area CA1 and the fascia dentata after destruction of CA3-CA4 afferents with kainic acid. Brain Res. 1980b; 182:1–9. [PubMed: 7350980]

Nusser Z, Lujan R, Laube G, Roberts JDB, Molnar E, Somogyi P. Cell type and pathway dependence of synaptic AMPA receptor number and variability in the hippocampus. Neuron. 1998; 21:545–559. [PubMed: 9768841]

Obenaus A, Esclapez M, Houser CR. Loss of glutamate decarboxylase mRNA-containing neurons in the rat dentate gyrus following pilocarpine-induced seizures. J Neurosci. 1993; 13:4470–4485. [PubMed: 8410199]

Okazaki MM, Evenson DA, Nadler JV. Hippocampal mossy fiber sprouting and synapse formation after status epilepticus in rats: visualization after retrograde transport of biocytin. J Comp Neurol. 1995; 352:515–534. [PubMed: 7721998]

Okazaki MM, Molnár P, Nadler JV. Recurrent mossy fiber pathway in rat dentate gyrus: synaptic currents evoked in presence and absence of seizure-induced growth. J Neurophysiol. 1999; 81:1645–1660. [PubMed: 10200201]

Palop JJ, Chin J, Roberson ED, Wang J, Thwin MT, Bien-Ly N, Yoo J, Ho KO, Yu G-Q, Kreitzer A, Finkbeiner S, Noebels JL, Mucke L. Aberrant excitatory neuronal activity and compensatory remodeling of inhibitory hippocampal circuits in mouse models of Alzheimer's disease. Neuron. 2007; 55:697–711. [PubMed: 17785178]

Parent JM, Yu TW, Leibowitz RT, Geschwind DH, Sloviter RS, Lowenstein DH. Dentate granule cell neurogenesis is increased by seizures and contributes to aberrant network reorganization in the adult rat hippocampus. J Neurosci. 1997; 17:3727–3738. [PubMed: 9133393]

Patrylo PR, Van den Pol AN, Spencer DD, Williamson A. NPY inhibits glutamatergic excitation in the epileptic human dentate gyrus. J Neurophysiol. 1999; 82:478–483. [PubMed: 10400974]

Peters, A.; Palay, SL.; Webster, H. The fine structure of the nervous system. Third Edition. Oxford University Press; New York: 1991.

Racine RJ. Modification of seizure activity by electrical stimulation. II. Motor seizure. Electroencephalogr Clin Neurophysiol. 1972; 32:281–294. [PubMed: 4110397]

Represa A, Jorquera I, Le Gal La Salle G, Ben-Ari Y. Epilepsy induced collateral sprouting of hippocampal mossy fibers: does it induce the development of ectopic synapses with granule cell dendrites? Hippocampus. 1993; 3:257–268. [PubMed: 8353609]

Sandler R, Smith AD. Coexistence of GABA and glutamate in mossy fiber terminals of the primate hippocampus: an ultrastructural study. J Comp Neurol. 1991; 303:177–192. [PubMed: 1672874]

Sassoé-Pognetto M, Panzanelli P, Sieghart W, Fritschy J-M. Colocalization of multiple $GABA_A$ receptor subtypes with gephyrin at postsynaptic sites. J Comp Neurol. 2000; 420:481–493. [PubMed: 10805922]

Sayin U, Osting S, Hagen J, Rutecki P, Sutula T. Spontaneous seizures and loss of axo-axonic and axo-somatic inhibition induced by repeated brief seizures in kindled rats. J Neurosci. 2003; 23:2759–2768. [PubMed: 12684462]

Schwarzer C, Williamson JM, Lothman EW, Vezzani A, Sperk G. Somatostatin, neuropeptide Y, neurokinin B and chole–cystokinin immunoreactivity in two chronic models of temporal lobe epilepsy. Neuroscience. 1995; 69:831–845. [PubMed: 8596652]

Schwarzer C, Tsunashima K, WanzenBöck C, Fuchs K, Sieghart W, Sperk G. $GABA_A$ receptor subunits in the rat hippocampus. II. Altered distribution in kainic acid-induced temporal lobe epilepsy. Neuroscience. 1997; 80:1001–1017. [PubMed: 9284056]

Scimemi A, Schorge S, Kullmann DM, Walker MC. Epileptogenesis is associated with enhanced glutamatergic transmission in the perforant path. J Neurophysiol. 2006; 29:1213–1220. [PubMed: 16282203]

Shao L-R, Dudek FE. Changes in mIPSCs and sIPSCs after kainate treatment: evidence for loss of inhibitory input to dentate granule cells and possible compensatory responses. J Neurophysiol. 2005; 94:952–960. [PubMed: 15772233]

Shi L, Argenta AE, Winseck AK, Brunso-Bechtold JK. Stereological quantification of GAD-67-immunoreactive neurons and boutons in the hippocampus of middle-aged and old Fischer 344x brown Norway rats. J Comp Neurol. 2004; 478:282–291. [PubMed: 15368530]

Simbürger E, Plaschke M, Kirsch J, Nitsch R. Distribution of the receptor-anchoring protein gephyrin in the rat dentate gyrus and changes following entorhinal cortex lesion. Cereb Cortex. 2000; 10:422–432. [PubMed: 10769252]

Simbürger E, Plaschke M, Fritschy J-M, Nitsch R. Localization of two major $GABA_A$ receptor subunits in the dentate gyrus of the rat and cell type-specific up-regulation following entorhinal cortex lesion. Neuroscience. 2001; 102:789–803. [PubMed: 11182243]

Sloviter RS. Decreased hippocampal inhibition and a selective loss of interneurons in experimental epilepsy. Science. 1987; 235:73–76. [PubMed: 2879352]

Sloviter RS. Possible functional consequences of synaptic reorganization in the dentate gyrus of kainate-treated rats. Neurosci Lett. 1992; 137:91–96. [PubMed: 1625822]

Sloviter RS, Sollas AL, Barbaro NM, Laxer KD. Calcium-binding protein (calbindin-D28K) and parvalbumin immunocytochemistry in the normal and epileptic human hippocampus. J Comp Neurol. 1991; 308:381–396. [PubMed: 1865007]

Sloviter RS, Dean E, Sollas AL, Goodman JH. Apoptosis and necrosis induced in different hippocampal neuron populations by repetitive perforant path stimulation in the rat. J Comp Neurol. 1996a; 366:516–533. [PubMed: 8907362]

Sloviter RS, Dichter MA, Rachinsky TL, Dean E, Goodman JH, Sollas AL, Martin DL. Basal expression and induction of glutamate decarboxylase and GABA in excitatory granule cells of the rat and monkey hippocampal dentate gyrus. J Comp Neurol. 1996b; 373:593–618. [PubMed: 8889946]

Somogyi P, Hodgson AJ, Smith AD, Nunzi MG, Gorio A, Wu J-Y. Different populations of GABAergic neurons in the visual cortex and hippocampus of cat contain somatostatin-or cholecystokinin-immunoreactive material. J Neurosci. 1984; 4:2590–2603. [PubMed: 6149275]

Staley KJ, Soldo BL, Proctor WR. Ionic mechanisms of neuronal excitation by inhibitory $GABA_A$ receptors. Science. 1995; 269:977–981. [PubMed: 7638623]

Steward O. Topographic organization of the projections from the entorhinal area to the hippocampal formation of the rat. J Comp Neurol. 1976; 167:285–314. [PubMed: 1270625]

Sun C, Mtchedlishvili Z, Bertram EH, Erishir A, Kapur J. Selective loss of dentate hilar interneurons contributes to reduced synaptic inhibition of granule cells in an electrical stimulation-based animal model of temporal lobe epilepsy. J Comp Neurol. 2007; 500:876–893. [PubMed: 17177260]

Sundstrom LE, Brana C, Gatherer M, Mepham J, Rougier A. Somatostatin- and neuropeptide Y-synthesizing neurons in the fascia dentata of humans with temporal lobe epilepsy. Brain. 2001; 124:688–697. [PubMed: 11287369]

Sutula T, Cascino G, Cavazos J, Parada I, Ramirez L. Mossy fiber synaptic reorganization in the epileptic human temporal lobe. Ann Neurol. 1989; 26:321–330. [PubMed: 2508534]

Thind KK, Ribak CE, Buckmaster PS. Synaptic input to dentate granule cell basal dendrites in a rat model of temporal lobe epilepsy. J Comp Neurol. 2008; 509:190–202. [PubMed: 18461605]

Trommald M, Hulleberg G. Dimensions and density of dendritic spines from rat dentate granule cells based on reconstructions from serial electron micrographs. J Comp Neurol. 1997; 377:15–28. [PubMed: 8986869]

Tsou K, Mackie K, Sanñudo-Penña MC, Walker JM. Cannabinoid CB1 receptors are localized primarily on cholecystokinin-containing GABAergic interneurons in the rat hippocampal formation. Neuroscience. 1999; 93:969–975. [PubMed: 10473261]

Turski L, Cavalheiro EA, Sieklucka-Dziuba M, Ikonomidou-Turski C, Czuczwar SJ, Turski W. Seizures produced by pilocarpine: neuropathological sequelae and activity of glutamate decarboxylase in the rat forebrain. Brain Res. 1986; 398:37–48. [PubMed: 3801899]

Vicario-Abejón C, Collin C, McKay RDG, Segal M. Neurotrophins induce formation of functional excitatory and inhibitory synapses between cultured hippocampal neurons. J Neurosci. 1998; 18:7256–7271. [PubMed: 9736647]

Wasterlain CG, Shirasaka Y, Mazarati AM, Spigelman I. Chronic epilepsy with damage restricted to the hippocampus: possible mechanisms. Epilepsy Res. 1996; 26:255–265. [PubMed: 8985705]

Wenzel HJ, Woolley CS, Robbins CA, Schwartzkroin PA. Kainic acid-induced mossy fiber sprouting and synapse formation in the dentate gyrus of rats. Hippocampus. 2000; 10:244–260. [PubMed: 10902894]

West MJ, Slomianka L, Gundersen HJG. Unbiased stereological estimation of the total number of neurons in the subdivisions of the rat hippocampus using the optical fractionator. Anat Rec. 1991; 231:482–497. [PubMed: 1793176]

Williams PA, White AM, Clark S, Ferraro DJ, Swiercz W, Staley KJ, Dudek FE. Development of spontaneous recurrent seizures after kainate-induced status epilepticus. J Neurosci. 2009; 29:2103–2112. [PubMed: 19228963]

Wittner L, Maglóczky Z, Borhegyi Z, Halász P, Tóth S, Eröss L, Szabó Z, Freund TF. Preservation of perisomatic inhibitory input of granule cells in the epileptic human dentate gyrus. Neuroscience. 2001; 108:587–600. [PubMed: 11738496]

Wuarin J-P, Dudek FE. Excitatory synaptic input to granule cells increases with time after kainate treatment. J Neurophysiol. 2001; 85:1067–1077. [PubMed: 11247977]

Yuan W, Matthews RT, Sandy JD, Gottschall PE. Association between protease-specific proteolytic cleavage of brevican and synaptic loss in the dentate gyrus of kainate-treated rats. Neuroscience. 2002; 114:1091–1101. [PubMed: 12379262]

Zhang W, Buckmaster PS. Dysfunction of the dentate basket cell circuit in a rat model of temporal lobe epilepsy. J Neurosci. 2009; 29:7846–7856. [PubMed: 19535596]

Zhang N, Houser CR. Ultrastructural localization of dynorphin in the dentate gyrus in human temporal lobe epilepsy: a study of reorganized mossy fiber synapses. J Comp Neurol. 1999; 405:472–490. [PubMed: 10098940]

Zhu Z-Q, Armstrong DL, Hamilton WJ, Grossman RG. Disproportionate loss of CA4 parvalbumin-immunoreactive interneurons in patients with Ammon's horn sclerosis. J Neuropathol Exp Neurol. 1997; 56:988–998. [PubMed: 9291940]

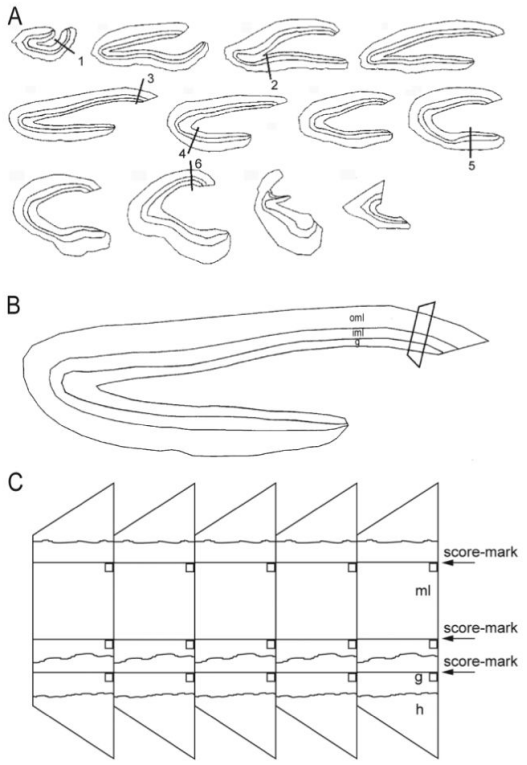

Figure 1.

Sampling scheme for stereological analysis of synapse numbers in the dentate gyrus. **A:** Starting from a random section near the septal pole, a 1-in-12 series of 40-μm-thick transverse sections was embedded. Cumulative length of the granule cell layer was measured and divided by 6. Sample sites along the granule cell layer were identified, starting at a random site in the first interval and at equal distances thereafter, designated by lines 1–6. **B:** Enlarged view of the section that includes sample site 3 in panel A. Areas of the granule cell layer (g), inner third of the molecular layer (iml), and outer two-thirds of the molecular layer (oml) were measured. Tissue at each sample site was trimmed into a trapezoid and mounted for ultrathin sectioning. **C:** Ribbons of ultrathin sections included the hilus (h), granule cell layer (g), and molecular layer (ml). Randomly located score-marks and edges of sections were used to place counting frames (squares) across aligned regions of serial sections.

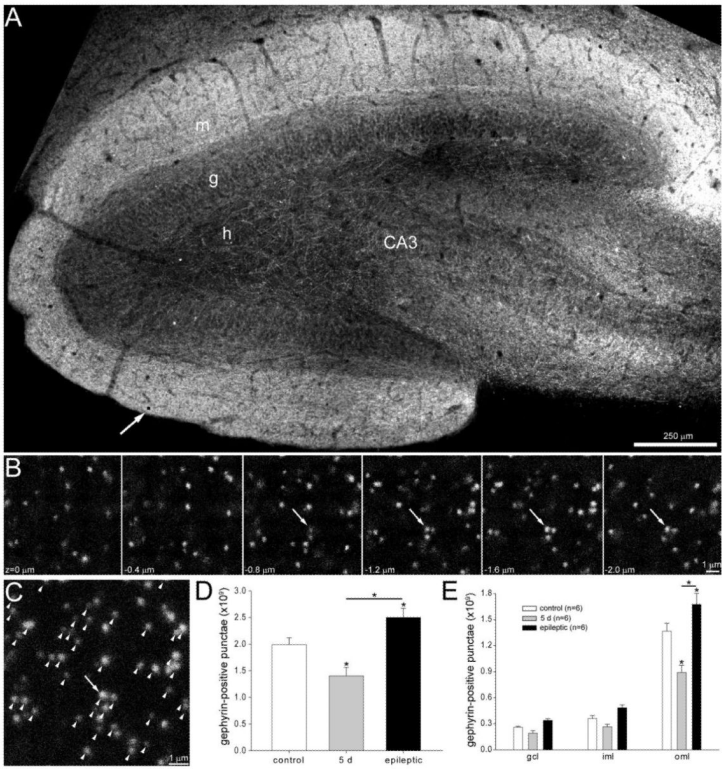

Figure 2.

Gephyrin-immunoreactive punctae numbers in the dentate gyrus decrease shortly after status epilepticus but later rebound and exceed control levels in epileptic rats. **A:** Gephyrin immunoreactivity in the dentate gyrus of an epileptic rat. h, hilus; g, granule cell layer; m, molecular layer; CA3, CA3 pyramidal cell layer. An arrow indicates one of the 9.2 × 9.2 μm counting frames (black square) in this section. **B:** A typical series of optical sections collected at the sample point indicated by the arrow and square in panel A. Punctae were counted if they were not visible in the most superficial section (z = 0 μm) and did not touch top or left borders. Arrows indicate a cluster of punctae that were counted. **C:** A composite image of the stack of optical sections shown in B. Arrow indicates the cluster of punctae identified in panel B. Arrowheads indicate all counted punctae. **D:** Numbers of gephyrin-positive punctae per dentate gyrus (not hilus) were reduced 5 days after status epilepticus and increased later in epileptic rats. Asterisks indicate differences from the control value, unless specified by a bar, which indicates a difference between rats 5 days after status epilepticus and epileptic animals ($P < 0.05$, ANOVA, Student–Newman–Keuls method). Values indicate mean ± SEM. **E:** Numbers of gephyrin-positive punctae by strata of dentate gyrus. gcl, granule cell layer; iml, inner molecular layer; oml, outer molecular layer.

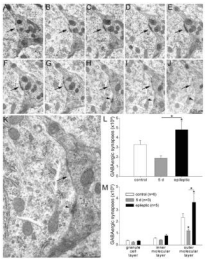

Figure 3.

GABA-immunoreactive synapse numbers per dentate gyrus (not hilus) decrease shortly after status epilepticus but later rebound and exceed control levels in epileptic rats. **A**–**J:** A series of consecutive electron micrographs showing an axo-somatic synapse (arrow) in the granule cell layer of a control rat. A second axo-somatic synapse becomes apparent in panel H (arrowhead). **K:** High-magnification view of panel H reveals 10-nm-diameter colloidal gold particles over GABA-immunoreactive axon terminals. **L:** Numbers of GABA-immunoreactive synapses per dentate gyrus (not hilus) were reduced 5 days after status epilepticus and increased later in epileptic rats. Asterisks indicate differences from the control value, unless specified by a bar, which indicates a difference between rats 5 days after status epilepticus and epileptic animals ($P < 0.05$, ANOVA, Student–Newman–Keuls method). Values indicate mean ± SEM. **M:** Numbers of GABA-immunoreactive synapses by strata of dentate gyrus. Largest changes were in the outer molecular layer.

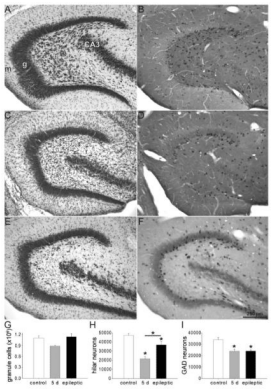

Figure 4.

Dentate gyrus stained with thionin (**A,C,E**) and processed for in situ hybridization for glutamic acid decarboxylase (**B,D,F**) in a control rat (A,B), a rat 5 days after status epilepticus (C,D), and an epileptic rat (E,F). h, hilus; g, granule cell layer; m, molecular layer; CA3, CA3 pyramidal cell layer. Numbers of granule cells (**G**), hilar neurons (**H**), and GABAergic interneurons (**I**) per dentate gyrus in controls, rats 5 days after status epilepticus, and epileptic rats. Asterisks indicate differences from the control value, unless specified by a bar, which indicates a difference between rats 5 days after status epilepticus and epileptic animals ($P < 0.05$, ANOVA, Student–Newman–Keuls method). Values indicate mean ± SEM $n = 6$, 3, and 5 rats for control, 5 days after status epilepticus, and epileptic groups, respectively.

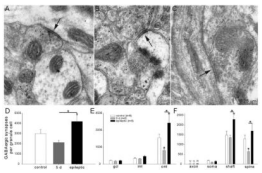

Figure 5.

GABA-immunoreactive synapses with putative granule cells. **A:** An axo-shaft GABAergic synapse (arrow) in the outer molecular layer of an epileptic rat. GABA-immunoreactivity is evident by 10-nm-diameter colloidal gold particles. **B:** An axo-spinous GABAergic synapse (arrow) in the outer molecular layer of an epileptic rat. **C:** An axo-axonic GABAergic synapse (arrow) in the granule cell layer of an epileptic rat. The axon initial segment is recognized by microtubules and dense membrane undercoating. **D:** Numbers of GABAergic synapses per granule cell were decreased 5 days after status epilepticus but later rebounded and exceeded control levels in epileptic rats. Asterisks indicate differences from the control value, unless specified by a bar, which indicates a difference between rats 5 days after status epilepticus and epileptic animals ($P < 0.05$, ANOVA, Student–Newman–Keuls method). Values indicate mean ± SEM. **E:** Numbers of GABAergic synapses per granule cell by strata of the dentate gyrus reveal largest reductions and later proliferations in the outer molecular layer. gcl = granule cell layer; iml = inner molecular layer; oml = outer molecular layer. F: Numbers of GABAergic synapses per granule cell by subcellular targets reveal most synapses with dendritic shafts and spines. Five days after status epilepticus, axo-spinous GABAergic synapse numbers were reduced most. In epileptic rats, axo-spinous and axo-shaft GABAergic synapses were increased most.

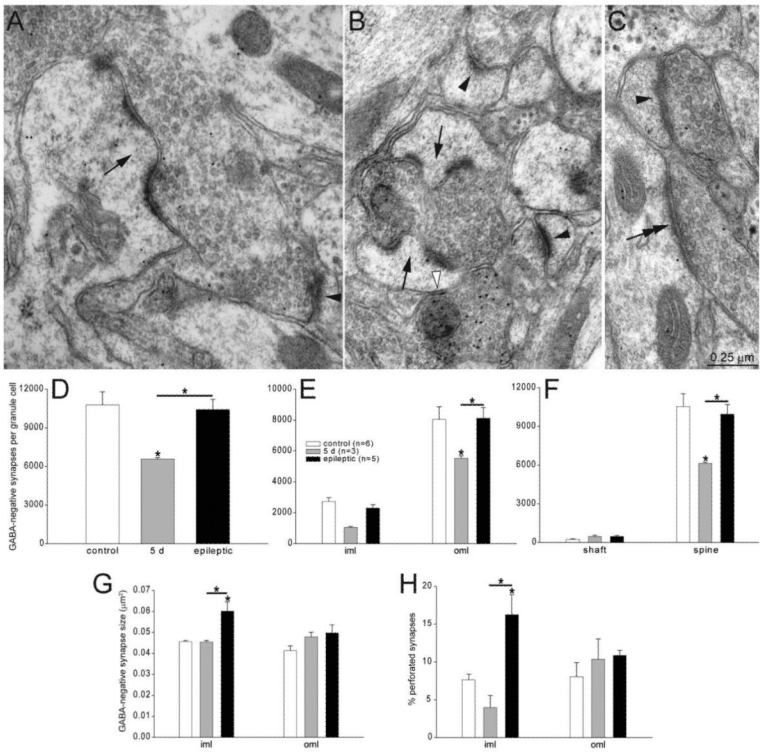

Figure 6.

GABA-negative synapses with putative granule cell dendrites in the molecular layer. **A:** A GABA-negative axon bouton forming a perforated synapse (arrow) with a GABA-negative dendritic spine in the inner molecular layer of an epileptic rat. A simple GABA-negative synapse with a spine is indicated by an arrowhead. **B:** A GABA-negative axon bouton forming perforated synapses (arrows) with GABA-negative dendritic spines in the inner molecular layer of an epileptic rat. Simple GABA-negative synapses with spines are indicated by black arrowheads. A GABA-positive synapse with a dendritic spine is indicated by a white arrowhead. GABA immunoreactivity is evident as concentrated 10-nm-diameter colloidal gold particles. **C:** A GABA-negative axon bouton synapsing with a GABA-negative dendritic shaft (double arrow) in the outer two-thirds of the molecular layer in a rat 5 days after status epilepticus. Another GABA-negative axon bouton forms a simple synapse with a dendritic spine (arrowhead). **D:** Numbers of GABA-negative synapses per granule cell were decreased 5 days after status epilepticus but later recovered to control levels in epileptic rats. iml = inner molecular layer; oml = outer molecular layer. Asterisks indicate differences from the control value, unless specified by a bar, which indicates a difference between rats 5 days after status epilepticus and epileptic animals ($P < 0.05$, ANOVA, Student–Newman–Keuls method). Values indicate mean ± SEM. **E:** Numbers of GABA-negative synapses per granule cell in the inner third (iml) and outer molecular layer (oml). **F:** Numbers of GABA-negative synapses per granule cell by subcellular targets reveal most synapses were with dendritic spines. Five days after status epilepticus, axo-spinous GABA-negative synapse numbers were reduced but recovered to control levels in epileptic animals. **G:** GABA-negative synapse size is increased in the inner molecular layer of epileptic rats. **H:** Percent of perforated synapses is increased in the inner molecular layer of epileptic rats.

TABLE 1

Primary Antibodies Used

Antigen	Immunogen	Manufacturer	Dilution
Gephyrin	Purified rat gephyrin	Synaptic Systems (Göttingen, Germany), mouse monoclonal, #147011	1:1,000
GABA	GABA conjugated to bovine serum albumin	Sigma (St. Louis, MO), rabbit polyclonal, #A2052	1:120

TABLE 2

Results and Parameters of Stereological Neuron and Punctae Counts in the Dentate Gyrus

	Nissl-stained hilar neurons	Nissl-stained granule cells	GAD-positive neurons[1]	Gephyrin-immunoreactive punctae[2]
Results				
Control	47,300 ± 2200	1.10 ± 0.06 (×10^6)	34,000 ± 1,900	1.99 ± 0.13 (×10^9)
5 d after status epilepticus	21,500 ± 2600	0.88 ± 0.03 (×10^6)	23,900 ± 1,800	1.40 ± 0.16 (×10^9)
Epileptic	36,800 ± 3600	1.14 ± 0.09 (×10^6)	24,100 ± 1,100	2.50 ± 0.17 (×10^9)
Parameters				
Sections/rat	11.1 ± 0.2	11.1 ± 0.2	11.1 ± 0.2	9.0 ± 0.2
Counting grid size (μm)	100 × 100	200 × 200	100 × 100	400 × 400
Counting frame size (μm)	40 × 40	10 × 10	40 × 40	9.2 × 9.2
Dissector height	Section thickness	Section thickness	Section thickness	2.0 μm
Cells or punctae counted/rat	507 ± 41	224 ± 10	248 ± 20	3230 ± 373
Coefficient of variation	0.308	0.164	0.218	0.286
Mean coefficient of error[3]	0.085	0.050	0.058	0.046

Values indicate mean ± SEM unless specified otherwise. Nissl- and GAD-stained sections were from one set of animals: n = 6, 3, and 5 rats for controls, 5 days after status epilepticus, and epileptic rats. Gephyrin data were obtained from a different set of rats: n = 6/group. Please refer to Figures 2 and 4 for results of statistical tests.

[1] Entire dentate gyrus (hilus, granule cell layer, and molecular layer) analyzed.

[2] Regions analyzed included granule cell layer and molecular layer, not hilus.

[3] Calculated according to West et al. (1991).

TABLE 3

Parameters of Stereological Electron Microscopic (EM) Synapse Counts in the Dentate Gyrus

Thick sections/rat	11.2 ± 2
EM sample sites/rat	6
Counting frame size (μm)	3.69 × 5.11
Dissector height (# ultrathin sections)	
Granule cell layer	150
Inner third molecular layer	100
Outer two-thirds molecular layer	100
No. ultrathin sections/thick section	813 ± 26
GABA-positive synapses counted/rat	1167 ± 103
GABA-negative synapses counted/rat	3073 ± 184
GABA-negative synapse sizes measured/rat	226 ± 12

Values indicate mean ± SEM unless specified otherwise. Data were collected from 14 rats: six controls, three at 5 days after status epilepticus, and five epileptic animals.